Article

Cell Reports

16p11 Duplication Disrupts Hippocampal-Orbitofrontal-Amygdala Connectivity, Revealing a Neural Circuit Endophenotype for Schizophrenia

Graphical Abstract

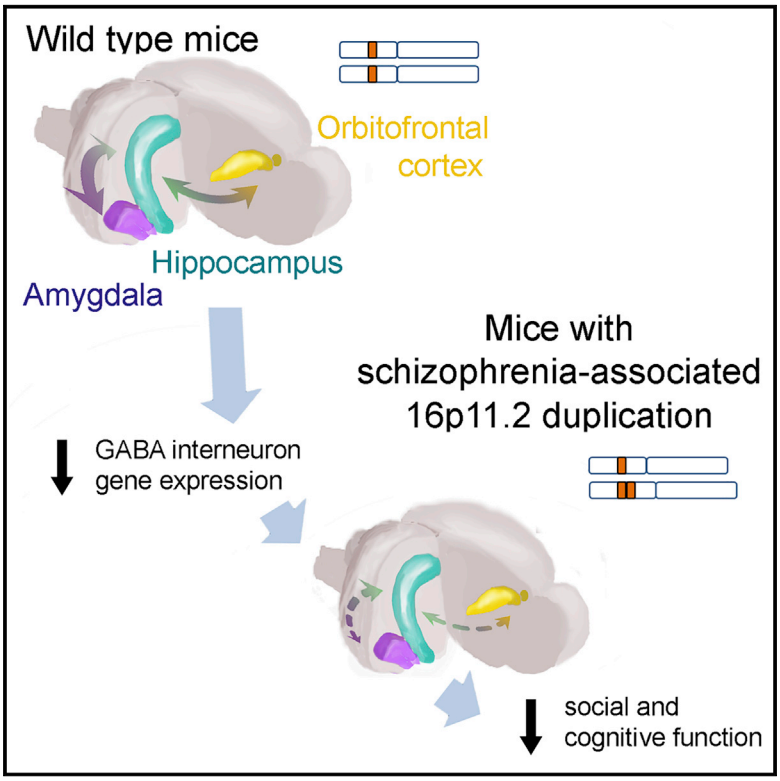

Authors

Greg C. Bristow, David M. Thomson, Rebecca L. Openshaw, Emma J. Mitchell, Judith A. Pratt, Neil Dawson, Brian J. Morris

Correspondence

brian.morris@glasgow.ac.uk

In Brief

Chromosome 16p11.2 duplications dramatically increase schizophrenia risk. In this study, Bristow et al. show that the mutation in mice suppresses GABAergic neuron gene expression, disrupts activity in hippocampal-orbitofrontal-amygdaloid circuitry, and compromises sociability and cognitive function. This supports the concept that impairment of this network is a core component of schizophrenia.

Highlights

- Mice reproducing the schizophrenia-associated 16p11.2 duplication are characterized
- The mutation disrupts hippocampal-orbitofrontal cortex-amygdala connectivity
- The mutation suppresses parvalbumin and somatostatin expression in these regions
- This is accompanied by impaired social/cognitive function in translational tests

Bristow et al., 2020, Cell Reports *31*, 107536
April 21, 2020
https://doi.org/10.1016/j.celrep.2020.107536

CellPress

Cell Reports
Article

16p11 Duplication Disrupts Hippocampal-Orbitofrontal-Amygdala Connectivity, Revealing a Neural Circuit Endophenotype for Schizophrenia

Greg C. Bristow,[1,4] David M. Thomson,[2,4] Rebecca L. Openshaw,[3,4] Emma J. Mitchell,[2,4] Judith A. Pratt,[2,5] Neil Dawson,[1,5] and Brian J. Morris[3,5,6,*]

[1]Department of Biomedical and Life Sciences, University of Lancaster, Lancaster LA1 4YW, UK
[2]Strathclyde Institute of Pharmacy and Biomedical Sciences, University of Strathclyde, Glasgow G4 0RE, UK
[3]Institute of Neuroscience and Psychology, College of Medical, Veterinary and Life Sciences, University of Glasgow, West Medical Building, Glasgow G12 8QQ, UK
[4]These authors contributed equally
[5]These authors contributed equally
[6]Lead Contact
*Correspondence: brian.morris@glasgow.ac.uk
https://doi.org/10.1016/j.celrep.2020.107536

SUMMARY

Chromosome 16p11.2 duplications dramatically increase risk for schizophrenia, but the mechanisms remain largely unknown. Here, we show that mice with an equivalent genetic mutation (16p11.2 duplication mice) exhibit impaired hippocampal-orbitofrontal and hippocampal-amygdala functional connectivity. Expression of schizophrenia-relevant GABAergic cell markers (parvalbumin and calbindin) is selectively decreased in orbitofrontal cortex, while somatostatin expression is decreased in lateral amygdala. When 16p11.2 duplication mice are tested in cognitive tasks dependent on hippocampal-orbitofrontal connectivity, performance is impaired in an 8-arm maze "N-back" working memory task and in a touchscreen continuous performance task. Consistent with hippocampal-amygdala dysconnectivity, deficits in ethologically relevant social behaviors are also observed. Overall, the cellular/molecular, brain network, and behavioral alterations markedly mirror those observed in schizophrenia patients. Moreover, the data suggest that 16p11.2 duplications selectively impact hippocampal-amygdaloid-orbitofrontal circuitry, supporting emerging ideas that dysfunction in this network is a core element of schizophrenia and defining a neural circuit endophenotype for the disease.

INTRODUCTION

Available drug treatments for schizophrenia (SZ) are effective against the positive symptoms (hallucinations, delusions), at least in the majority of patients, but are largely ineffective against the negative (anhedonia, avolition, self-neglect, social withdrawal) and cognitive (impaired working memory [WM] and attention) symptoms. Development of improved treatments will only be enabled by increased understanding of the causes of the disease and how they impact on neurobiology, and by better preclinical models of facets of the disease.

The genetic architecture of SZ is complex (Giegling et al., 2017). Many common sequence variations interact to increase disease risk, although each common variant individually has only a very small effect. It is therefore extremely challenging to design rodent genetic models of the disease with high construct validity, as any individual disease risk genetic variant, of very small effect, is likely to have a relatively small disease-relevant impact on CNS function. However, it is now clear that in rare cases, single human copy-number variants (CNVs), where small chromosomal sections are present in one or three instead of two copies, can dramatically perturb CNS function on their own and substantially increase disease risk. Of these CNVs, the 22q11 (velocardiofacial/DiGeorge Syndrome) deletion CNV has received considerable attention, as it substantially increases risk of SZ (penetrance 6.5–18 [95% confidence interval, CI]) (Kirov et al., 2014). A number of 22q11 mouse models have consequently been developed to study the impact of this CNV on CNS function, and, promisingly, impaired hippocampal-prefrontal synchrony has been reported (Sigurdsson et al., 2010). Due to the relative difficulty of designing translatable behavioral assays for positive and negative symptoms of the disorder, the resulting genetically modified (GM) mice are commonly tested in cognitive tasks chosen to reflect the cognitive deficits observed in patients with SZ. A difficulty is that the 22q11 CNV is also associated with generalized cognitive impairment and intellectual disability (ID) in almost all patients. Hence, when mice modeling the 22q11 deletion are assessed in cognitive tasks, any deficits observed are likely to reflect aspects of general ID, rather than a specific SZ-related impairment.

Other CNVs have been identified more recently that also profoundly increase SZ risk. The 16p11.2 locus is attracting special interest as, rather surprisingly, it is associated with reciprocal risks for psychiatric and neurodevelopmental

Table 1. Alterations in Regional Centrality in 16p11.2 DUP Mice

Region	Centrality Measure	WT	16p11.2 Duplication
Hippocampus			
Ventral hippocampus CA3 (VH-CA3)	Eigenvector	2.08	−1.02*
Ventral hippocampus DG (VH-DG)	Eigenvector	2.05	−2.65***
Basal Ganglia			
Substantia nigra pars reticulata	Eigenvector	2.04	−2.66***
Substantia nigra pars compacta	Betweenness	5.08	−0.72*
Amygdala			
Central amygdala	eigenvector	2.04	−1.36**
Mesolimbic			
Nucleus accumbens core	betweenness	5.34	−0.13*
Septum			
Lateral septum	betweenness	6.73	−0.52*
Sensory			
Somatosensory cortex	betweenness	8.08	−0.42**
Auditory			
Medial geniculate	betweenness	4.47	−0.59*

[1]Regions considered to be functional hubs in the brain networks ($Z > 1.96$).
Data shown as the Z score centrality measure within each group, calculated by comparison to 11,000 calibrated Erdös-Rényi random networks. *$p < 0.05$, **$p < 0.01$, and ***$p < 0.001$ indicate significant difference from WT mice (55,000 permutations of the data).

disorders. Carriers of a deletion at this locus have an increased risk of autism-spectrum disorders (ASDs) and IDs, but not SZ (Cooper et al., 2011; Stefansson et al., 2014, 2008; Weiss et al., 2008). In fact the 16p11.2 *deletion* is among the most common genetic variants in ASDs (Weiss et al., 2008). In contrast, a high proportion of 16p11.2 *duplication* (16p11.2 DUP) carriers develop SZ (Kirov et al., 2014; Marshall et al., 2017; McCarthy et al., 2009; Rees et al., 2014; Vassos et al., 2010; Zheng et al., 2013), but only a small proportion also have IDs (Cooper et al., 2011), and do not generally show ASDs. The proportion of 16p11.2 DUP carriers developing SZ appears to be similar to that of 22q11 deletion carriers (penetrance 4.3–14) (Kirov et al., 2014; Marshall et al., 2017), but since the 16p11.2 DUP increases risk of ID much less than the 22q11 deletion, the phenotypic effects are more specific to SZ (Kirov et al., 2014). In fact, the 16p11.2 DUP represents one of the most powerful genetic risk factors known for SZ (Marshall et al., 2017).

The genomic organization at this locus in the mouse is comparable to that in humans, allowing the generation of GM mice with an equivalent (chr. 7F3) syntenic duplication (16p11.2 DUP mice) (Arbogast et al., 2016; Horev et al., 2011). The 16p11.2 DUP mice are without any overt behavioral phenotype, but reportedly show subtle hypoactivity (Arbogast et al., 2016; Horev et al., 2011). In this study, we utilize a range of translational parameters that can be equated with clinical measures (Pratt et al., 2012, 2018) to explore the neurobiological impact of the CNV, and to assess the extent to which 16p11.2 DUP mice exhibit functional abnormalities that resemble characteristics of patients with SZ. The findings have considerable significance for future exploration of the neurobiological basis of the disease, and for translational studies attempting to bridge the preclinical-clinical barriers to drug development.

RESULTS

Altered Functional Brain Network Connectivity in 16p11.2 Mice

Advances in imaging technologies and analytical methods, including network science and related algorithms, have revealed alterations in functional brain network connectivity in SZ. One of the most consistent endophenotypes reported in SZ includes a reduction in hippocampal-prefrontal cortex (PFC) connectivity (Dawson et al., 2015b; Godsil et al., 2013; Sakurai et al., 2015). There is some evidence that individual SZ risk genes/CNVs (Dawson et al., 2015a; Sigurdsson et al., 2010) also impact on functional brain network structure and hippocampal-PFC connectivity in mice. We have therefore examined the properties of functional brain networks of 16p11.2 DUP mice.

16p11.2 DUP mice exhibited selective alterations in constitutive cerebral metabolism limited to the serotonergic raphé, and the striatum (Figure S2), showing significant hypometabolism in the median raphé (MR) nucleus ($p = 0.032$, ANOVA), and hypermetabolism in the dorsolateral striatum (DLST, $p = 0.003$, ANOVA) and ventromedial striatum (VMST, $p = 0.015$, ANOVA).

Hub Brain Region Status Is Altered in the Functional Brain Networks of 16p11.2 DUP Mice

We found that regional functional connectivity was significantly altered in 16p11.2 DUP mice, in terms of both regional importance (centrality) and inter-region functional connectivity (partial least-squares regression (PLSR) analysis).

Regional importance in these functional brain networks was characterized using centrality analysis (degree [K_c], betweenness [B_c], Eigenvector [E_c]). Many of the brain regions identified as important functional hubs in the brain networks of wild-type (WT) animals were lost in 16p11.2 DUP mice. This included the

loss of hub regions in the ventral hippocampus (cornu ammonis 3 [VH-CA3] and dentate gyrus [VH-DG] subfields), the central amygdala nucleus (CeA), and the substantia nigra (pars compacta [SNc] and pars reticulata [SNr]). In addition, the nucleus accumbens core (AcbC) and the lateral septum (LS) were identified as significant hubs in the functional brain networks of WT mice that were significantly lost in those of 16p11.2 DUP mice (Table 1). Two other brain regions, the medial geniculate (MG; part of the auditory thalamus) and the primary somatosensory (S1) cortex, also lost hub status in the functional brain networks of 16p11.2 DUP mice. This suggests that the organization of functional brain networks is profoundly altered in 16p11.2 DUP mice. Full centrality data are shown in Table S2.

Despite these regional changes in functional connectivity, when characterized at the global scale, we found that the properties of functional brain networks in 16p11.2 DUP mice were not significantly altered in comparison to those in WT animals. Functional networks in 16p11.2 DUP mice showed a similar number of total functional connections (mean degree, $< k >$), and had a similar average pathlength (L_p). There appeared to be decreased clustering (Cp) in the brain networks of 16p11.2 DUP mice, but this did not reach statistical significance ($p = 0.060$, Figure S3).

PLSR Analysis Identifies Compromised Hippocampal, Basal Ganglia, Amygdala, and Prefrontal Cortex Functional Connectivity in 16p11.2 DUP Mice

Given the loss of functional hub brain regions in the brain networks of 16p11.2 DUP mice (Table 1), we sought to characterize the alterations in inter-regional functional connectivity underlying these losses. Therefore we employed the PLSR algorithm to define the functional connectivity of these "seed" brain regions, as previously described (Dawson et al., 2013, 2015a).

When the CA3 and DG subfields of the VH were used as seed regions of interest (ROIs) in PLSR analysis, the evidence supported the significant loss of functional connectivity of these hippocampal regions to multiple other hippocampal subfields (DH-CA1, DH-CA2, DH-DG, VH-CA3, VH-DG, and VH-MoL), the amygdala (CeA and medial amygdala [MeA]), and the PFC (lateral orbital cortex [LO] subfield) in 16p11.2 DUP mice (abbreviations detailed in Table S1).)

When the CeA was considered as the seed ROI, we found evidence for significantly lost connectivity to multiple hippocampal subfields (DH-CA1, DH-CA2, VH-CA3, VH-DG, and entorhinal cortex [ENT]), thalamic nuclei (anterior thalamic reticular nucleus [aTRN]), mediodorsal thalamus [MD], and ventromedial thalamus [VM]), and the SNR in 16p11.2 DUP mice. When the AcbC was considered as the seed region, a significant decrease in functional connectivity to the hippocampus (VH-DG, VH-MoL, and ENT), basal ganglia (SNr and globus pallidus [GP]), and the PFC (Cg1 and LO) was observed in 16p11.2 DUP mice (Figure 1).

When the substantia nigra (SNc and SNr) were considered as seed brain ROI in the analysis, there was reduced connectivity to the hippocampus (DH-CA1, DH-DG, VH-CA3, Ent, and perirhinal cortex [PRh]), the CeA, nucleus accumbens (AcbS), and the striatum (dorsolateral striatum - DLST and ventromedial striatum - VMST) in 16p11.2 DUP mice. These effects were seen for the SNR but not for the SNc, which showed altered connectivity to the retrosplenial cortex (RSc), MG, and habenula (Hab) in 16p11.2 DUP mice (Figure 1).

In addition to these alterations, the differences in LS, MG, and S1 cortex functional connectivity were also characterized in 16p11.2 DUP mice, again supporting compromised connectivity of these regions to the PFC, amygdala, and hippocampal subfields (Figure 1). Overall, these data support altered hippocampal, amygdala, basal ganglia, and prefrontal functional connectivity as a result of 16p11.2 DUP. Full data are shown in Table S2.

Any correlation between the regional functional activity of individual mice and their behavioral phenotype would be of significant interest. Therefore, we assessed the extent to which locomotor activity (LMA) in an open field correlated with regional cerebral metabolism in WT and 16p11.2 DUP mice (Figure S4). In WT mice, cerebral metabolism in select subfields of the frontal cortex (mPrL and dorsolateral orbital cortex [DLO]) and VH (VH-CA1 and VH-MoL) was strongly related to LMA (Figure S4). In addition, activity in the S1 and insular (Ins) cortices was strongly related to LMA in WT mice, as was metabolism in the GP and olfactory bulb (OB). Metabolism in many of the same brain regions, including the DLO and Ins, was found to be strongly related to LMA in 16p11.2 DUP mice. However, some regions defined as being important to LMA in WT mice (e.g., VH-CA1, OB, and medial prelimbic cortex [mPrL]) were not defined as being related to LMA in 16p11.2 mice (Figure S4). By contrast, metabolism in multiple brain regions was strongly and significantly related to LMA in 16p11.2 DUP but not WT mice. This included metabolism in multiple cortical (LO and piriform cortex [Piri]), thalamic (anteromedial [AM] and reticular nucleus [TRN]), and hippocampal (DH-MoL, dorsal subiculum [DSub], and VH-DG) regions. In addition, cerebral metabolism in the SNr, ventral limb of the diagonal band of Broca (VDB), and CeA was strongly related to LMA in 16p11.2 DUP but not WT mice. Intriguingly, many of the regions identified as showing an altered contribution to LMA in 16p11.2 DUP mice were hub regions whose functional connectivity was significantly altered in the brain networks of these animals (Figure 1; Table 1). This includes the CeA and DH-MoL, VH-DG, MG, S1, and SNR that were identified as important functional hubs in the brains of WT mice that significantly lost their hub connectivity status in 16p11.2 DUP mice. Overall, this suggests that dysfunction in regions showing altered functional connectivity in 16p11.2 DUP mice is related to their behavioral phenotype.

We noted some effects of sex on the network properties and functional connectivity measures (Figure S5; Table S4). A number of brain regions were identified as being significant hubs in the functional brain networks of female but not in male mice (Table S2). This included the AM (eigenvector centrality) and anteroventral (AV) (eigenvector centrality) thalamus, the RSc (degree and eigenvector centrality), LS (betweenness centrality), and the molecular layer of the ventral hippocampus (VH-ML, betweenness centrality). In particular, there was evidence for reduced hippocampal-orbitofrontal connectivity in males compared to females (Figure S5). We also monitored brain size, and found reductions throughout the neuraxis in the 16p11.2 DUP mice, consistent with previous reports (Horev et al., 2011) (Figure S6).

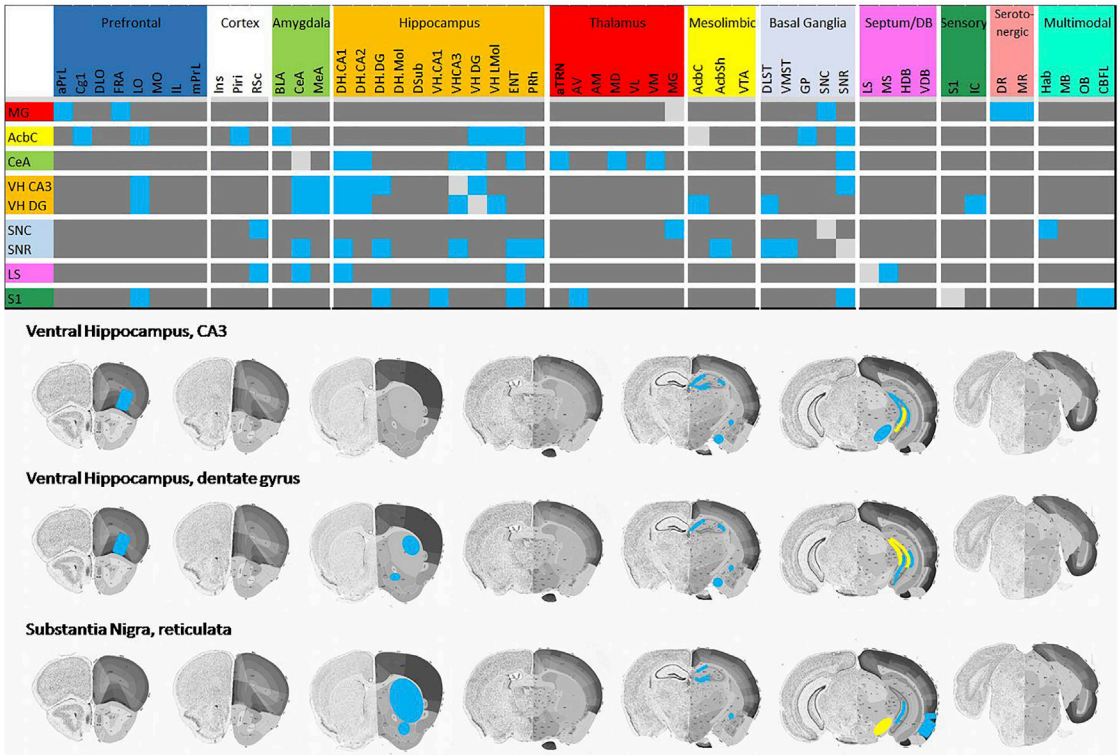

Figure 1. Changes in Regional Functional Connectivity of 16p11.2 DUP Mice

(Top panel) Heatmap showing functional connectivity of "seed" regions. Seed regions were identified based on a loss of hub status in centrality analysis and a significant difference in *Z* score in 16p11.2 DUP mice compared to the wild-type control group (Table 1). Light-blue panels indicate a significant (**Z < -2.98**) loss of functional connectivity between the highlighted brain regions in 16p11.2 DUP mice compared to wild-type controls, as determined by PLSR analysis.

(Bottom panel) Coronal images of the mouse brain showing the localization of decreased regional connectivity for selected seed regions in 16p11.2 DUP mice. Yellow denotes the location of the seed region; light blue denotes regions for which there has been a significant ($Z < -2.98$) loss of connectivity to the seed region in the 16p11.2 DUP mice as determined by PLSR analysis.

See Table S2 for full data of functional connectivity for all seed regions. See Table S1 for a full list of abbreviations. Mouse brain images are modified from the Allen Mouse Brain Atlas (http://mouse.brain-map.org/static/atlas). N = 6 males and 5 females per genotype.

Altered GABAergic Interneuron Gene Expression in Lost Functional Hubs in 16p11.2 DUP Mice

In light of the lost regional connectivity identified in 16p11.2 DUP mice, we next examined changes in GABAergic markers in these regions. Reduced parvalbumin (Pvalb), calbindin, and somatostatin (SST) expression in regions of the PFC and orbitofrontal cortex (OFC) are arguably the most robust neurochemical abnormality detected in post-mortem tissue from patients with SZ (Hashimoto et al., 2008; Hoftman et al., 2015). Thus, we characterized the regional expression of these genes in 16p11.2 DUP mice. We found that the CNV was associated with reduced expression of Pvalb and calbindin, in lateral OFC. SST mRNA levels were decreased in the infralimbic (IL) region of the PFC (Figure 2). *GAD1* (encoding GAD67) expression appeared unaffected in PFC and OFC regions, but was reduced in the TRN, where Pvalb and calbindin expression were also reduced (Figure 2). This is noteworthy, considering evolving theories that TRN dysfunction is an early event in the development of SZ (Pratt and Morris, 2015).

Having observed reduced hippocampal-amygdala connectivity in 16p11.2 DUP mice, we also probed for GABAergic gene expression deficits in the amygdala nuclei. Here, we detected decreased expression of calretinin mRNA in the medial amygdala, and decreased SST mRNA in the lateral amygdala (Figure 3).

Since the 16p11.2 DUP mice showed altered brain connectivity and gene expression changes across three primary systems—orbitofrontal-hippocampal, hippocampal-amygdala, and the basal ganglia—we then assessed performance in behavioral tasks that recruit these systems, and which are considered to have relevance to the positive, negative, and cognitive symptom domains of SZ (Pratt et al., 2012, 2018).

16p11.2 DUP Mice Are Hypoactive and Exhibit Altered Sensory Gating

We first examined if 16p11.2 DUP mice showed changes in a range of fundamental physical parameters (SHIRPA battery) that could influence performance in subsequent tests. No significant effects of 16p11.2 DUP genotype were detected (data not shown). We observed a (sex-dependent) reduction in LMA in an open-field arena (novel environment) (Figure 4A), with male 16p11.2 DUP mice showing a lower level of activity compared to male WT control mice. This is consistent with previous reports showing that 16p11.2 DUP mice show reduced levels of locomotion (Arbogast et al., 2016; Horev et al.,

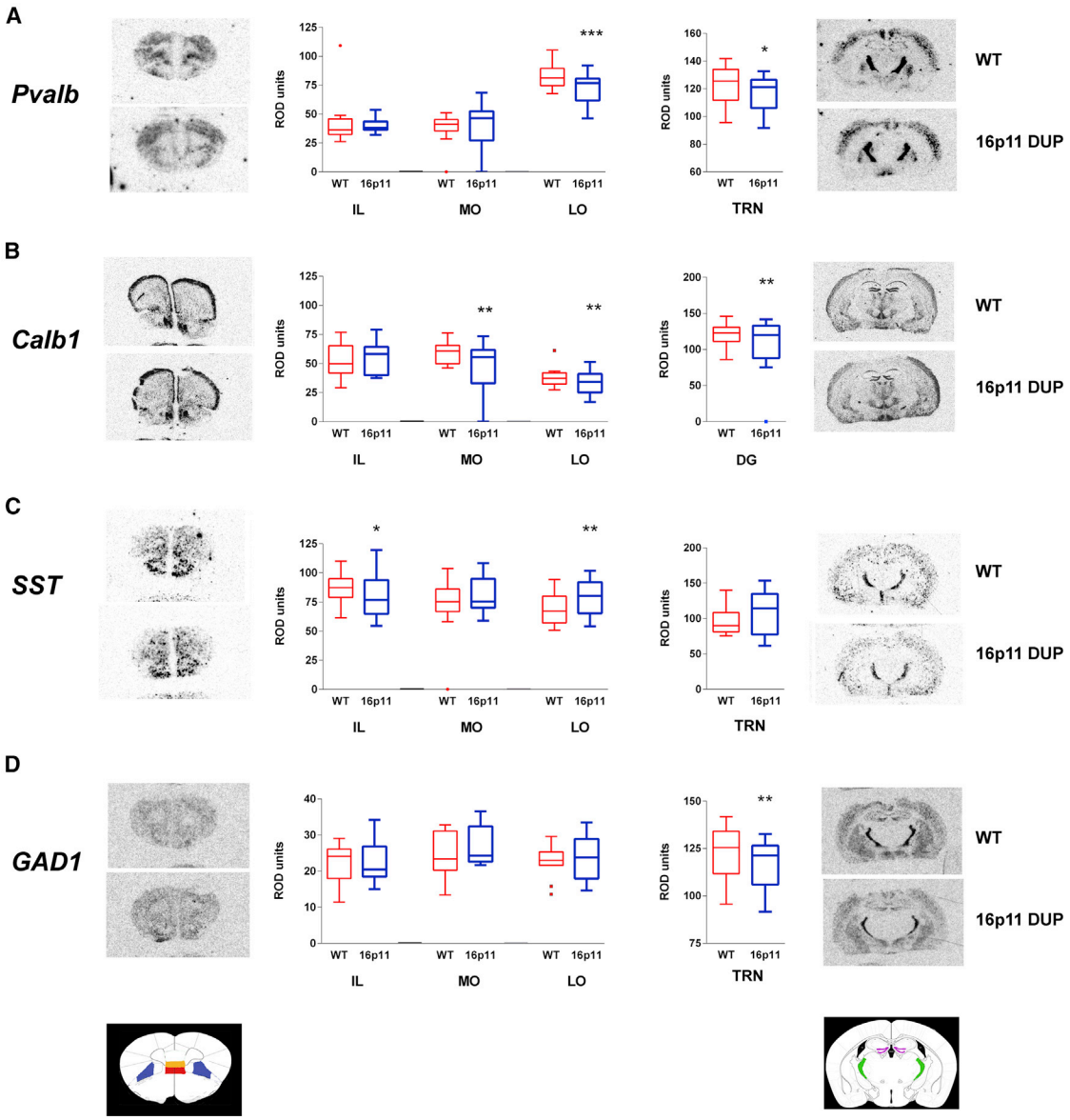

Figure 2. 16p11.2 Duplication Decreases GABAergic Interneuron Gene Expression in Orbitofrontal Cortex and Thalamus

(A–D) Example autoradiographs are shown at the level of the prefrontal cortex (left), and hippocampus and thalamus (right), with box-and-whisker plots showing group data.

(A) Parvalbumin (Pvalb).

(B) Calbindin (Calb1).

(C) Somatostatin (SST).

(D) Gad-67 (GAD1).

Boxplots show median with interquartile range and "Tukey" whiskers. Scale bar represents 2 mm. **$p < 0.01$ and *$p < 0.05$ (ANOVA) versus corresponding WT group. Schematic diagrams (bottom left and right) show location of infralimbic (IL) cortex (orange), medial orbitofrontal (MO) cortex (red), lateral orbitofrontal (LO) cortex (blue), hippocampal dentate gyrus (DG, purple), and thalamic reticular nucleus (TRN, green). N = 6 males and 6 females per genotype.

2011). While 16p11.2 DUP mice showed no change in basic startle amplitude in the prepulse inhibition (PPI) of the startle response test (Figure S7), there was evidence for a reduction in the PPI relative to WT mice (Figure 4D) (ANOVA $p = 0.05$) that was more pronounced in female mice (Figure 4D) (ANOVA $p = 0.008$).

16p11.2 DUP Mice Exhibit Altered Social and Emotional Behaviors

Impaired social functioning is a key feature of SZ, but there are limitations in capturing the complexity and multidimensional nature of this domain in rodent models (Millan and Bales, 2013). In part this is because existing rodent paradigms involve

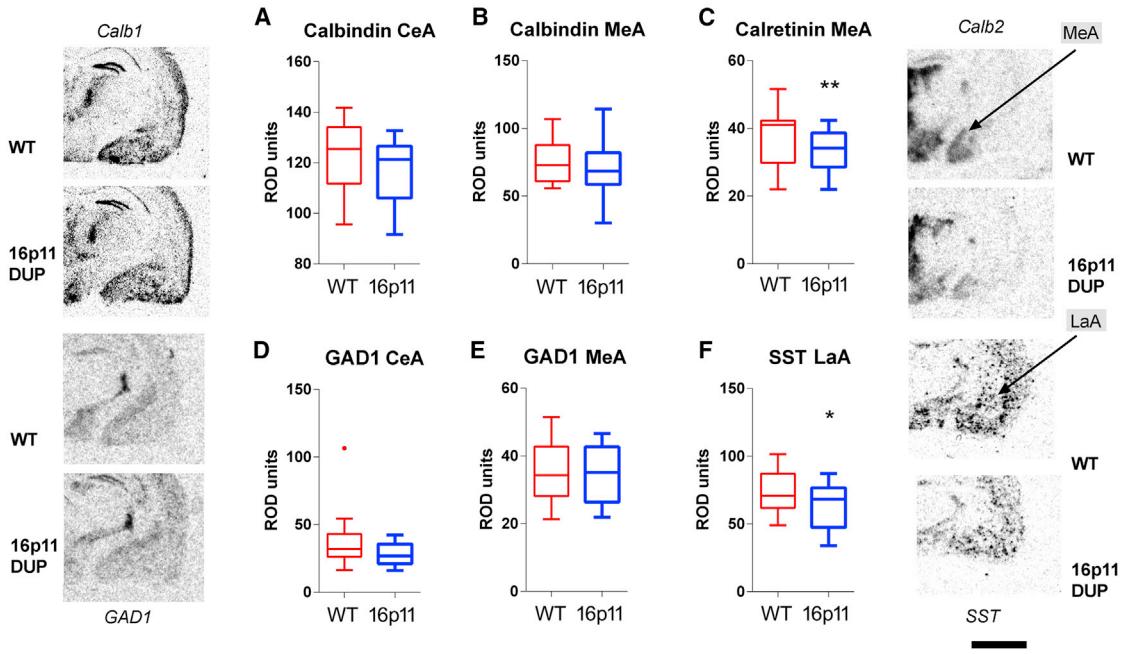

Figure 3. 16p11.2 Duplication Decreases SST and Calretinin Expression in Amygdala

(A–D) Example autoradiographs are shown at the level of the amygdala, with box-and-whisker plots showing group data.

(A and B) Calb1.

(C) Calretinin (*Calb2*).

(D and E) *GAD1*.

(F) *SST*.

N = 6 males and 6 females per genotype. Boxplots show median with interquartile range and Tukey whiskers. Scale bar represents 2 mm. $^{**}p < 0.01$ and $^{*}p < 0.05$ (ANOVA) versus corresponding WT group.

elements of stress responsivity, as behavior is monitored in a novel environment often between unfamiliar animals and only provides a snapshot of behavior over a limited time frame. We therefore monitored behaviors in group housed mice in a home-cage environment over a 3-day period. Mice showed typical circadian patterns of activity (being more active in the dark phase). Reduced LMA was again detected in 16p11.2 DUP mice, although this was more marked in female mice in this case (Figures 4E and 4F).

16p11.2 DUP mice also showed signs of social impairment. First, during the dark phase, average distance between cage-mates was increased in 16p11.2DUP mice relative to WT controls, and this genotype effect was more pronounced in males (Figure 4G). Furthermore, over a 3-day period, 16p11.2 DUP mice spent less time in close proximity (<50 mm) to cage-mates (Figure 4H). Average time spent in close proximity to cage-mates was reduced in 16p11.2 DUP mice, and this genotype effect was most prominent during the light phase (Figure 4I). Since changes in emotional behaviors may influence social functioning, we assessed whether 16p11.2 DUP mice showed anxiety-like behaviors in the elevated plus maze. Male, but not female, 16p11.2 DUP mice showed signs of increased anxiety-like behavior, spending less time in the open arms of an elevated plus maze (Figure 4C). They also spent a smaller proportion of time than their WT counterparts in the inner section of the open-field arena, indicating an aversion to explore a novel environment (Figure 4B).

We also looked to see if the pattern of behavior showed any sign of changing over the 3-day period of monitoring. For both locomotor and social measures, the phenotypes appeared stable over the 3 days of testing (Figure S7).

16p11.2 DUP Mice Exhibit Deficits in Hippocampal-Orbitofrontal Dependent Cognitive Tasks

Patients with SZ show a characteristic pattern of cognitive impairment, notably in tasks that involve hippocampal-orbitofrontal connectivity. We employed two behavioral tests designed to interrogate aspects of cognitive function that have cross-species commonalities in respect of neural circuitry, and hence maximize rodent-human translational potential. The human N-back task probes hippocampal-PFC-dependent short-term WM processes, and deficits in this task are present in patients with SZ (Meyer-Lindenberg et al., 2005; Schobel et al., 2009). The eight-arm maze WM task (WMT) is an adaption of the radial arm maze task that explores performance at increasing levels of WM load (Marighetto et al., 2008) that has translational relevance to the N-back WMT commonly used in patients. Thus, here we will refer to the task as the rodent "N-back" WMT.

Separate cohorts of mice were assessed at two ages—younger (10 weeks at start) and older (40 weeks at start). This task requires considerable training, and, as expected, there was a significant overall effect of training block ($p < 0.001$), with performance improving over the initial weeks,

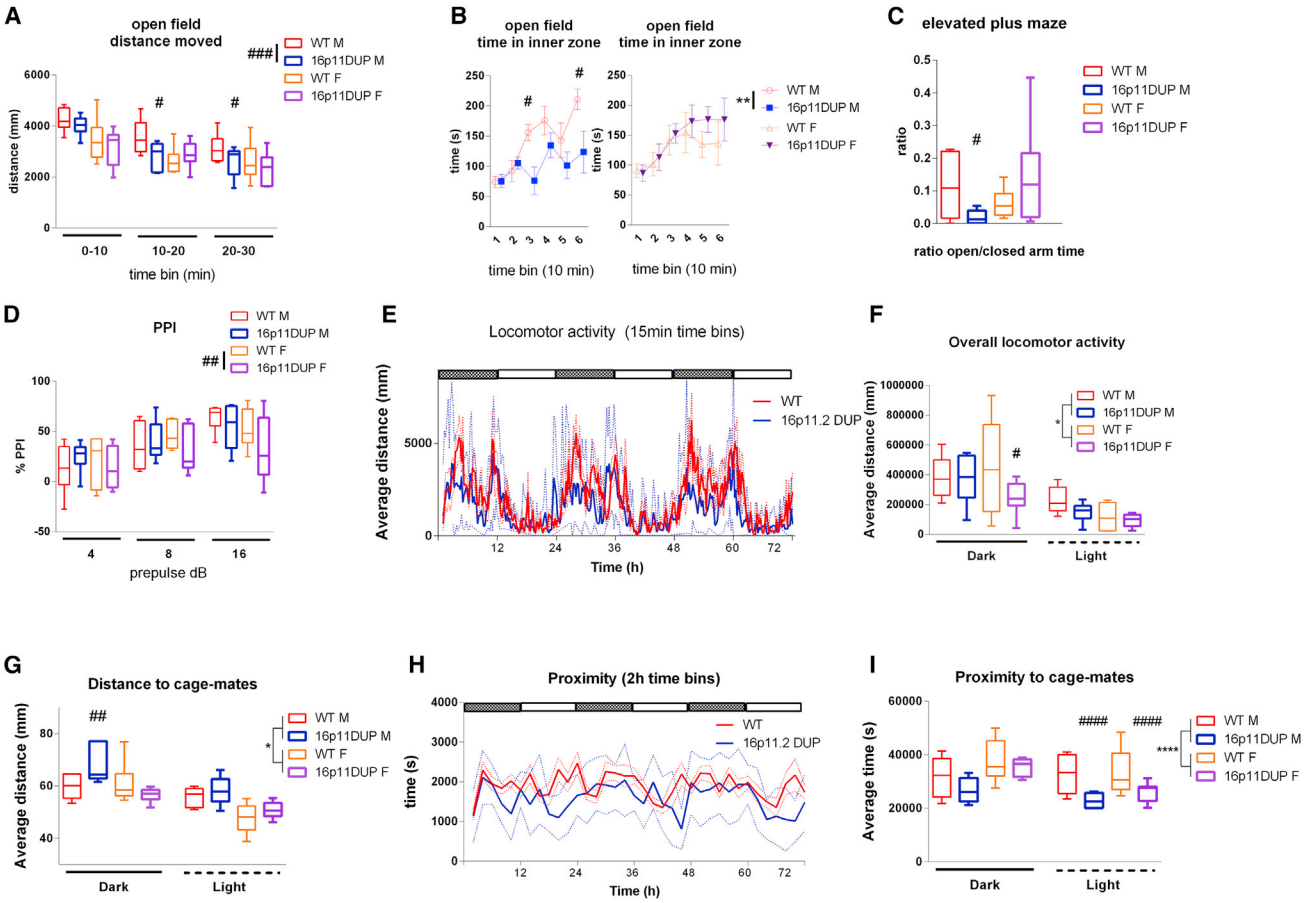

Figure 4. Effect of 16p11.2 Duplication in Mice on Behavior

(A–D) Behavior in a novel environment and sensory motor gating.

(A) Locomotor activity.

(B) Time in inner zone of open-field arena, for male (left) and female (right) mice, in an open-field arena.

(C) Elevated plus maze, ratio of time in open arm compared to time in closed arm.

(D) PPI.

(E–I) Ethological behavior in home-cage environment over 3 days.

(E) Locomotor activity over 3 days. Continuous lines indicate group means, dotted lines indicate mean ± SEM; dark and light bars indicate dark and light phases. Data shown for mixed sexes.

(F) Median distance traveled with interquartile range and Tukey whiskers.

(G) Median separation from cage-mates over 3 days, with interquartile range and Tukey whiskers.

(H) Proximity to cage-mates over 3 days, illustrated in the same way as (E).

(I) Median proximity with interquartile range and Tukey whiskers.

N = 6 males and 6 females (A–D) or 6 males and 9 females (E–H) per genotype. Data are shown either as mean ± SEM (B, E, and H), or as boxplots with median, interquartile range, and Tukey whiskers. ****p < 0.0001, ***p < 0.001, **p < 0.01, *p < 0.05 (ANOVA), #p < 0.05, ##p < 0.01, and ####p < 0.0001 versus corresponding WT group (post hoc Tukey test).

but then stabilizing such that no significant additional improvement was seen from training blocks 4 onward. As in the human task, levels of performance decreased with increasing WM load (increasing "n") (Figures 5A and 5B). There was an overall significant effect of age, with older mice performing less well than younger animals. There was a highly significant effect of genotype, independent of the age of the mice, with impaired performance in 16p11DUP mice (Figures 5A and 5B). Data from blocks 4–7, for both ages, were then pooled for increased clarity, showing the impaired performance in 16p11.2 DUP mice (Figure 5C). There was no significant interaction between 16p11.2 genotype and training block, indicating that while 16p11.2 DUP mice showed a significant deficit in WM performance, their ability to learn the task across sessions was similar to that seen in WT mice. There was, however, a highly significant ($p < 0.001$) interaction between age and training block, with the older mice learning less well over time.

The reaction time for each choice is not measured in this task, but total time to complete the task in each session was used as a proxy measure of reaction time. While the time taken decreased with training, 16p11DUP mice appeared slower than WT

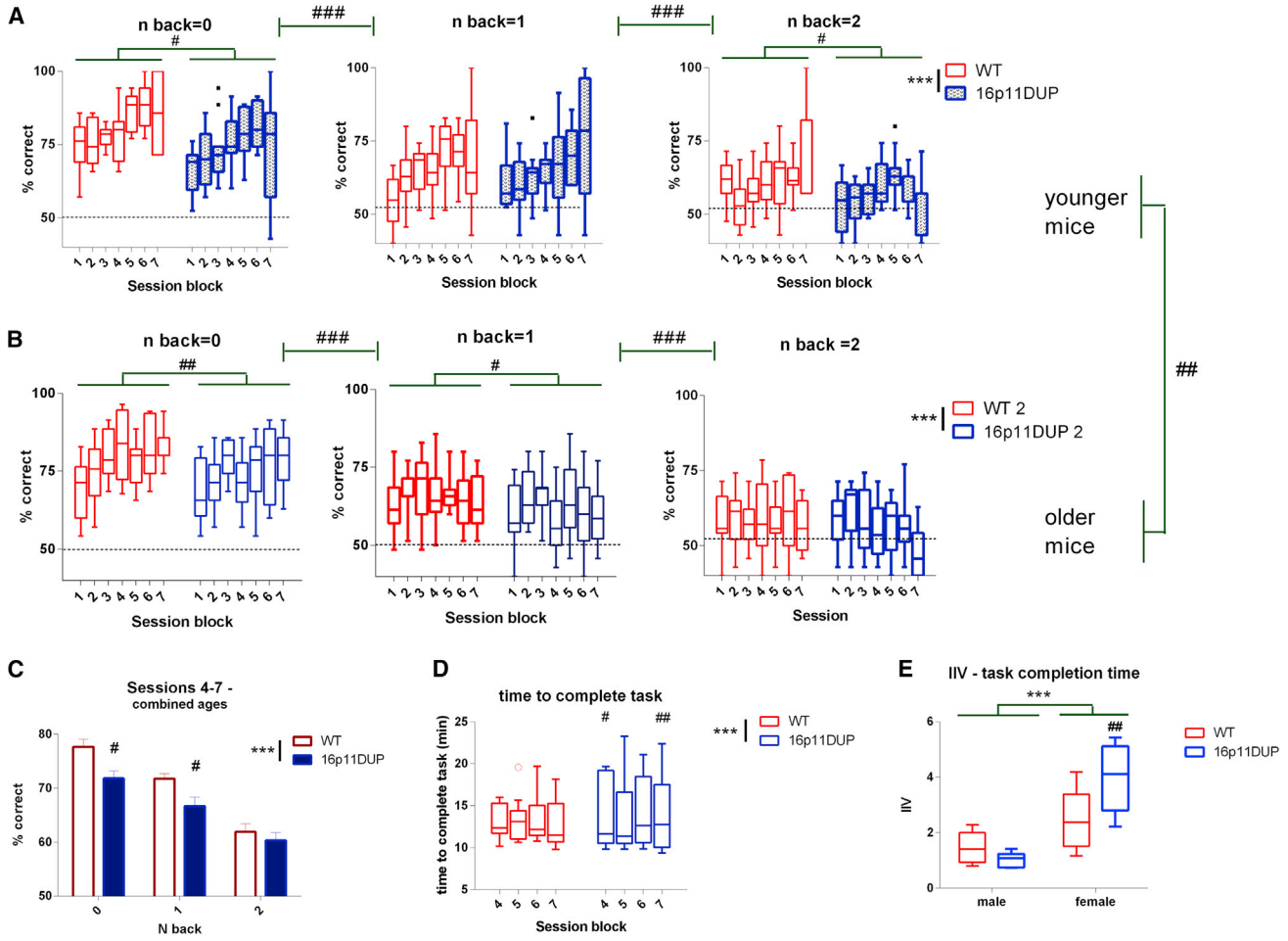

Figure 5. Effect of 16p11.2 Duplication in Mice on Performance in the N-back Task

(A and B) Task performance as % correct choices, across 5-day blocks of training sessions, in younger (A) or older (B) mice. Chance level of performance = 50%.

(C) Performance in training session blocks 4–7 with combined age groups.

(D) Time to complete task in younger mice, for blocks 4–7.

(E) Intra-individual variability (IIV) in younger mice for blocks 4–7.

N = 6 males and 6 females per genotype. Data are shown either as mean ± SEM, or as boxplots with median, interquartile range, and Tukey whiskers. Dots represent outliers. ***$p < 0.001$ (ANOVA), #$p < 0.05$, ##$p < 0.01$, and ###$p < 0.001$ versus corresponding WT group, or as indicated (post hoc Tukey test).

controls, reflecting much greater variability in completion time (Figure 5D).

One of the most robustly-observed cognitive abnormalities in patients with SZ is an increased intra-individual variability (IIV) in processing speed (PS) in WM and attentional tasks, including the N-back task (Cole et al., 2011; Manoach, 2003; Zhou et al., 2014). When we monitored the IIV for the proxy measure of total time to complete task, we observed a sex-specific effect, with female 16p11.2 DUP mice exhibiting greater IIV than WT females or males (Figure 5E).

The rodent continuous performance task (CPT) has been developed to mirror the widely-used human CPT, and employs touchscreen apparatus to maximize cross-species equivalence (Mar et al., 2013). Mice were trained according to Kim et al. (2015). In this task, mice were assessed for attentional performance (hit rate and false alarm rate), along with composite measures of performance according to receiver operating characteristics, analogous to the measures commonly used in clinical studies (perceptual sensitivity = d′ and index of response bias = response indices [RIs]), and PS (reaction time). Patients with SZ typically show reductions in d′, more liberal indices of response bias, and reduced PS (Elvevåg et al., 2000; Liu et al., 1997). Patients with 16p11.2 DUPs exhibit reduced PS (Stefansson et al., 2014).

During acquisition of the task, (e.g., stage 3), 16p11.2 DUP mice showed impaired performance, with lower hit rates and d′ values, but also with reduced false alarm rates and RIs (Figures 6A–6D). Once the task was fully acquired, performance of 16p11.2 DUP mice was similar to WT mice, with d′ slightly elevated, although RI values were substantially higher, indicative of more liberal, risky responding (Figures 6E and 6F)

16p11.2 DUP mice also showed PS deficits, as evidenced by slower reaction times (Figure 6G), although there was no indication of increased reaction time IIV in this task (Figure 6H).

DISCUSSION

The reason 16p11.2 duplications lead to dramatically enhanced risk of SZ, without generalized ID, is of intense interest. We demonstrate here that the CNV leads to a relatively selective dysfunction of hippocampal-orbitofrontal-amygdaloid circuitry, underpinned in part by GABAergic interneuron dysfunction, along with corresponding behavioral effects, which, in addition to reproducing aspects of the syndrome associated with 16p11.2 DUPs in humans, phenocopy many aspects of SZ itself.

We also found reduced brain size in 16p11.2 DUP mice, an observation consistent with previous reports of 16p11.2 DUP mice (Arbogast et al., 2016; Horev et al., 2011), and clinical reports in 16p11.2 patients (Steinman et al., 2016). However, despite the general reduction in brain size, the functional alterations are neuroanatomically restricted. This includes the loss of functional hub brain regions, paralleling the loss of functional and structural hub regions in SZ (Rubinov and Bullmore, 2013). We were intrigued to find that hippocampal-orbitofrontal networks were particularly affected by the CNV. There is a major afferent pathway to the OFC from the hippocampus (Barbas and Blatt, 1995; Godsil et al., 2013; Roberts et al., 2007). Only relatively recently has it been widely appreciated that orbitofrontal dysfunction is a core element of SZ (Godsil et al., 2013; Homayoun and Moghaddam, 2008). Structural changes in OFC are robustly observed in patients (Lacerda et al., 2007; Nakamura et al., 2008; Sanfilipo et al., 2000), and this pathway appears to become compromised at an early stage, as changes are detected in parallel with the onset of psychosis in at-risk populations, in parallel with cognitive impairment (Guo et al., 2014; Pantelis et al., 2003; Salvador et al., 2010). Patients with chronic SZ show clearly altered functional activity in hippocampal and orbitofrontal regions (Schobel et al., 2009), and actively hallucinating patients show elevated metabolic activity specifically in hippocampus and OFC (Silbersweig et al., 1995). Hippocampal-orbitofrontal-amygdaloid circuitry is also specifically implicated in thought disorder—viewed as a hallmark of SZ (Sumner et al., 2018). Our findings, that a major consequence of 16p11.2 DUP is compromised hippocampal-orbitofrontal connectivity, are consistent with the concept that dysfunction of this pathway can be a fundamental cause of SZ. Indeed, previous studies have reported OFC dysfunction in other genetic (Dawson et al., 2014a; Johnson et al., 2013) and pharmacological (Dawson et al., 2014b) rodent models relevant to the disorder.

Amygdala-hippocampal connectivity is profoundly involved with emotion, anxiety, and social engagement. A substantial literature describes amygdala-hippocampal dysfunction in psychiatric disease (discussed below).

GABAergic Molecular Alterations in 16p11.2 DUP Mice Parallel Changes Seen in Patients with SZ

Patients with SZ show reduced expression of Pvalb and SST in GABAergic interneurons in prefrontal and orbitofrontal cortices (Beasley and Reynolds, 1997; Hoftman et al., 2015; Fung et al., 2010; Hashimoto et al., 2008; Joshi et al., 2015; Morris et al., 2008). It is therefore extremely pertinent that the 16p11.2 CNV is sufficient to cause abnormal Pvalb and SST in prefrontal/orbitofrontal regions. Reduced calbindin expression is also reliably detected in post-mortem PFC from patients with SZ (Beasley et al., 2002). The observed decrease in calbindin mRNA in the medial orbital cortex is therefore also important. The lack of change in PFC/orbitofrontal calretinin expression is also broadly consistent with results in patient tissue (Beasley et al., 2002; Hoftman et al., 2015). It is notable that SST mRNA levels are also reduced in the lateral amygdaloid nucleus in 16p11.2 DUP mice, paralleling the reduced SST mRNA levels reported in the lateral amygdala in patients with SZ (Chang et al., 2017; Pantazopoulos et al., 2017).

Overall, genes within the 16p11.2 region clearly control SZ-relevant gene expression in prefrontal/OFC and amygdala. Interestingly, reduced activity in SST neurones of the IL cortex is sufficient to impair hippocampal-prefrontal synchrony (Abbas et al., 2018), so the reduced SST expression seen in the IL in 16p11.2 DUP mice (Figure 2) may contribute to the lost hippocampal-PFC connectivity (Figure 1) seen in these animals. However, it is also likely that the GABAergic interneuron alterations localized to the LO cortex of 16p11.2 DUP mice also play a key role in disrupting hippocampal-PFC connectivity in these animals.

Alterations in Social- and Anxiety-like Behavior in 16p11.2 DUP Mice Parallel those that are Seen in SZ and Align with Their Functional Brain Connectivity Deficits

Impaired social cognition in SZ is an important determinant of daily functioning and shows a strong relationship with positive and negative symptoms (Green et al., 2015; Millan and Bales, 2013). This multidimensional construct includes the capacity to detect, analyze, and interpret social signals from others, together with recognizing and understanding their beliefs, intentions, and actions (theory of mind). This ultimately permits appropriate social behaviors. Clearly, there are challenges in capturing elements of social cognition in rodents (Millan and Bales, 2013), although measuring spontaneous social interactions in rodents in a familiar home-cage environment offer considerable promise. We show that 16p11.2 DUP mice express reduced social interaction behaviors in a low-stress, home-cage testing environment. A range of interconnecting neural networks are involved in social cognition including the PFC, ventral striatum, amygdala, and cingulate cortex (Barak and Feng, 2016; Bicks et al., 2015; Grabenhorst et al., 2019). These neural systems all show compromised functional connectivity in 16p11.2 DUP mice. Furthermore, orbitofrontal-hippocampal connectivity has been specifically linked to cognitive processes relating to social interaction (Ross et al., 2013). Thus our findings of reduced connectivity among the OFC, amygdala, and hippocampus provide a mechanistic substrate for the social deficits observed in the 16p11.2 DUP mice.

Social behaviors are influenced by emotional states, such as anxiety. Notably, 16p11.2 DUP mice showed signs of increased anxiety, albeit modest, in the elevated plus maze and open-field test. This could potentially relate to a partially characterized neural circuitry encompassing hippocampus, amygdala, OFC, and raphé nuclei (Andrade et al., 2013; Shin and Liberzon, 2010). High anxiety is a feature of patients with 16p11.2 DUPs (Filges et al., 2014; Knoll et al., 2018; Martin-Brevet et al.,

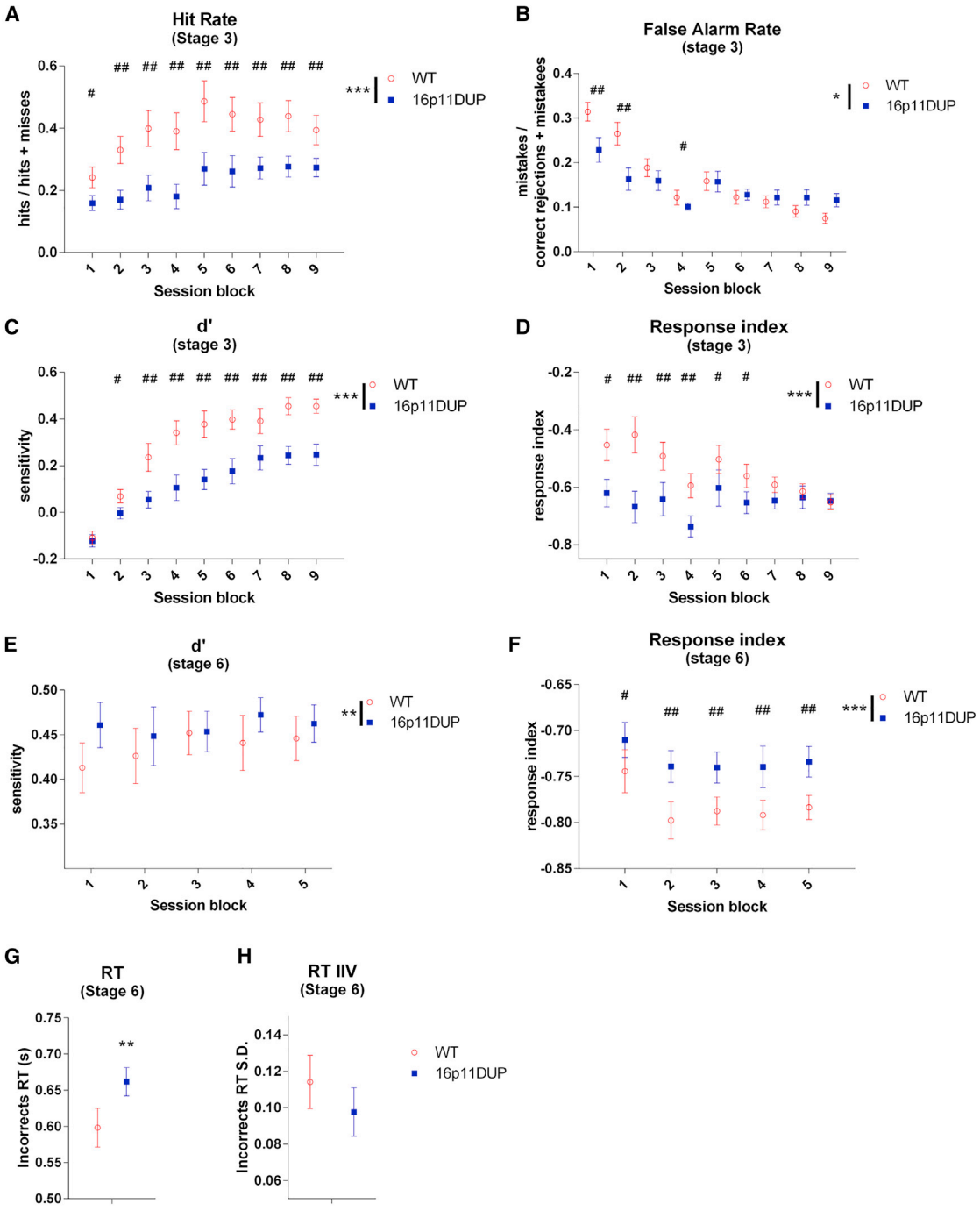

Figure 6. Effect of 16p11.2 Duplication in Mice on Performance in the Touchscreen rCPT

(A and B) HR (A) and FAR (B) at stage 3.

(A) HR Effect of genotype, $p < 0.001$.

(B) FAR Effect of genotype, $p = 0.021$.

(C and D) d′ (C) and RI (D) at stage 3.

(C) Stage 3 d′ effect of genotype, $p < 0.001$.

(D) Stage 3 response bias effect of genotype, $p < 0.001$.

(E and F) d′ (E) and RI (F) at stage 6.

(E) Stage 6 d′ effect of genotype, $p < 0.01$.

(F) Stage 6 response bias effect of genotype, $p < 0.001$.

(G and H) Reaction time incorrect responses (G) and reaction time IIV (H) at stage 6.

(legend continued on next page)

2018; Rosenfeld et al., 2010), and also patients with SZ (Achim et al., 2011).

The majority of the behavioral effects of the 16p11.2 DUP were observed independently of the sex of the mice. A few significant effects were sex dependent: while both males and females demonstrated reduced LMA, for females this was detected in the home-cage monitoring, while for males this was detected in the novel environment of the open-field arena. This suggests that phenotype manifestation in the different sexes is potentially affected by additional factors, notably the level of stress. The novel environment will involve additional stress compared to the home cage, and indeed male 16p11.2 DUP mice seem more sensitive than females to anxiety-inducing situations, as exemplified by the results in the elevated plus maze (Figure 4). In this context, it is interesting that we found evidence for reduced hippocampal-orbitofrontal connectivity in males compared to females (Figure S6), raising the possibility that males are therefore more prone to the effect of the duplication to heighten anxiety. Supporting the contribution of additional factors to the observed sex-dependent phenotypes, both male and female 16p11.2 DUP mice showed reduced home-cage social interaction, but for females this was apparent only for the separation-distance measure, whereas it was detectable for both sexes on the proximity-time measure (Figure 4).

16p11.2 DUP Mice Show Deficits in Cognition Relevant to Those Seen in Human Individuals with the 16p11.2 Duplication and Patients with SZ

SZ is typically associated with a specific profile of cognitive dysfunction encompassing deficits in executive processes including WM (e.g., N-back task), cognitive flexibility, and attention (e.g., CPT). 16p11.2 DUP carriers (without co-morbid SZ), show a relatively selective impairment in spatial WM and reduced psychomotor PS, without affecting attention or cognitive flexibility (as reflected by the degree of perseveration) (Stefansson et al., 2014)—suggesting that, without effects related to the development of SZ, the cognitive impairments are relatively limited in individuals with 16p11.2 DUPs.

The cognitive changes identified here in 16p11.2 DUP mice strongly align with those reported in humans with 16p11.2 DUPs. For example, the performance of 16p11.2 DUP mice is compromised in the N-back WM task, where they generate a reduced number of correct responses compared to WT mice. There is a spatial component to the mouse (maze-based) N-back task, and hence the impairments in mice may be related to the deficits in spatial WM seen in human 16p11.2 DUP carriers.

Increased IIV is also a robust finding in SZ patients (Shin et al., 2013), and has been linked to OFC function (Albaugh et al., 2017). We noted evidence suggesting increased IIV in N-back task performance in female 16p11.2 DUP mice. Indeed, in humans, IIV is greater in females than males in WM tasks (Dykiert et al., 2012).

Interestingly, hippocampal-orbitofrontal dysconnectivity is sufficient to cause these deficits. Orbitofrontal-hippocampal functional connectivity is strengthened (Zald et al., 2014) during performance of the N-back task in humans, and OFC lesions compromise WM task performance in monkeys and humans (Barbey et al., 2011; Iversen and Mishkin, 1970). Hence our observation of GABAergic interneuron deficits in OFC and impaired connectivity with hippocampus may explain the impaired performance in the N-back task in 16p11.2 DUP mice. These observations also parallel the reduced hippocampal-PFC connectivity in another mouse model of a CNV relevant to SZ—the 22q11.2 mouse model—linked to deficits in a WM test equivalent to N-back n = 0 in the test used here (Sigurdsson et al., 2010). Amygdaloid connectivity may also be important, as a growing literature also implicates lateral OFC-amygdala connections in value assessment of rewarding experience (Chau et al., 2015; Malvaez et al., 2019).

Consistent with relatively spared attentional performance in human 16p11.2 DUP carriers, 16p11.2 DUP mice performed comparatively well in the CPT, despite some impaired performance during task acquisition, and more risky responding once the task was established. Interestingly, mice with a genetic manipulation mirroring the 22q11 deletion CNV show similar impairment at stage 3 of the CPT, with reduced hit rate and increased false alarms (Nilsson et al., 2016)—although, consistent with the more generalized ID associated with this CNV in humans, they also show impaired hit rate at stage 6.

Patients with SZ are impaired in the CPT, showing reduced hit rates and d′, along with elevated false alarm rates, generally more impulsive responding, and slower reaction times (Fleck et al., 2001). These characteristics were strikingly reproduced in the touchscreen CPT in 16p11.2 DUP mice. In the CPT, the 16p11.2 DUP mice are slower to learn the task. Although ultimately they achieve relatively normal levels of performance in terms of hit rate, they continue to show more risky responding strategies. Note that while higher RI values are indicative of more liberal responding (Kim et al., 2015), this is the converse of the complementary LnBeta index used clinically, where low values indicate more liberal responding strategies.

The altered GABAergic interneuron gene expression and functional connectivity we have detected in 16p11.2 DUP mice may be directly responsible for the cognitive impairment. In general, the role of the OFC, and especially lateral OFC, is most commonly defined in terms of restraint and response inhibition (Dias et al., 1996; Elliott et al., 2000), with OFC dysfunction typically leading to increased false alarm rates. OFC activity increases during response inhibition, a phenomenon increased in SZ (Schirmbeck et al., 2015). In fact, a highly-selective impairment of OFC Pvalb cells is sufficient to cause such

(G) Reaction time for incorrect responding.

(H) IIV for incorrect responding reaction time.

N = 6 males and 6 females per genotype. Data are shown as mean ± SEM. *p<0.05, **p<0.01,***p < 0.001 (ANOVA), #p < 0.05, and ##p < 0.01 versus corresponding WT group (post hoc Tukey test).

cognitive deficits (Goodwill et al., 2018) (increased false-responding during cognitive challenge).

The Role of Individual 16p11.2 Genes in SZ-Relevant Phenotypes

Although there are ~30 genes within the human CNV, some insight is available into the contribution of specific genes to the phenotypes observed. It should be noted that the mouse strain used here has a duplication of these and also three additional genes (*Cd2bp2*, *Tbc1d10b*, and *Sept1*). Although these three genes are not part of the core duplication in humans, they reportedly also show elevated expression in tissues from human 16p11.2 DUP carriers (Blumenthal et al., 2014). While they do represent a slight variation from the human mutation, where there is commonality between the assays that we have used and those used by Arbogast et al. (2016) (brain size, LMA) in which the mouse duplication more exactly matches the human core duplication, we note that there is good correspondence between the two strains of mice. In terms of 16p11.2 genes and neurobiological *sequelae*, the microencephaly phenotype is reproduced in zebrafish as a result of KCTD13 overexpression (but not of other 16p11.2 genes) (Golzio et al., 2012). ERK1 is important for many aspects of cognitive function, so *Mapk3* duplication may contribute to the cognitive phenotypes we report. Increased LMA in *Mapk3* knockout mice (Mazzucchelli and Brambilla, 2000; Selcher et al., 2001) implicates duplication of this gene in the hypolocomotor phenotype. However, *Mapk3* knockout mice show normal PPI and anxiety behavior (Selcher et al., 2001). It has recently become clear that c-jun N-terminal kinase (JNK) signaling makes a substantial contribution to the regulation of anxiety (Mohammad et al., 2018; Stefanoska et al., 2018), with a lack of JNK being anxiolytic. Mice with a genetic deletion specifically of the *Taok2* gene exhibit reduced anxious behavior in a novel environment (Richter et al., 2019), linking Taok2 to anxiety mechanisms. Since *TAOK2* is an upstream activator of JNK, the hyper-anxiety in (male) 16p11.2 DUP mice can potentially be ascribed to the duplication of the *Taok2* gene within the CNV. Mice lacking *Taok2* also show hyperlocomotion (Richter et al., 2019), so the hypoactive phenotype of 16p11.2 DUP mice may also result from increased *Taok2* gene dosage. Much future work is needed to dissect the specific relationships that exist between single genes in the 16p11.2 region, or potential synergistic interactions between these genes, and the generation of translationally relevant phenotypes.

Synthesis of Findings

The overall picture that emerges from these studies is that the 16p11.2 DUP impacts on hippocampal-orbitofrontal and hippocampal-amygdala pathways. The results are consistent with data emerging from other murine genetic models of rare, high-penetrance SZ risk, and also with some recent evidence from 16p11.2 deletion mice. It will be important to build on this knowledge, to understand the role of specific genes within the CNV in the rather anatomically specific disruption of function. The SZ-relevant behavioral deficits that we have detected are all consistent with reduced prefrontal/orbitofrontal expression of SST and Pvalb, and compromised hippocampal-orbitofrontal communication. Interestingly, OFC Pvalb cells are particularly sensitive to early-life stress (Goodwill et al., 2018), so the poorly-characterized interactions with environmental risk may also converge on this pathway. Here we show deficits in hippocampal-orbitofrontal-amygdalar circuity that are accompanied by deficits in cognitive subdomains and social deficits in highly translatable tasks. Importantly, this "circuitry-cellular and behavioral" phenotype closely aligns with deficits observed in patients with duplications in 16p11.2. Thus, the data provide insight into how the CNV affects cognition, and increases the risk of developing SZ, in humans. Furthermore, the data support the use of 16p11.2 DUP mice as a model of high construct validity, with translational phenotypes, which can be utilized for future drug development studies.

STAR★METHODS

Detailed methods are provided in the online version of this paper and include the following:

- KEY RESOURCES TABLE
- LEAD CONTACT AND MATERIALS AVAILABILITY
- EXPERIMENTAL MODEL AND SUBJECT DETAILS
  - Animals
- METHOD DETAILS
  - In Situ Hybridization
  - 14C-2-Deoxyglucose Imaging
  - Network Analysis using Graph Theory Algorithms
  - Partial Least-Squares Regression (PLSR)
  - Using PLSR Analysis to Define Altered Relationships between Regional Cerebral Metabolism and Locomotor Activity (LMA) in 16p11.2 DUP Mice
  - Gross Morphology
  - Open Field Arena
  - Elevated Plus Maze
  - PPI
  - N Back Radial Maze Task
  - CPT
  - Home Cage Monitoring
- QUANTIFICATION AND STATISTICAL ANALYSIS
- DATA AND CODE AVAILABILITY

SUPPLEMENTAL INFORMATION

Supplemental Information can be found online at https://doi.org/10.1016/j.celrep.2020.107536.

ACKNOWLEDGMENTS

This research was supported by the Medical Research Council (UK) grant MR/N012704/1.

AUTHOR CONTRIBUTIONS

D.M.T., G.C.B., R.L.O., and E.J.M. performed the experiments, conducted most of the data analysis, and contributed to writing the manuscript. J.A.P., N.D., and B.J.M. conceived the study, provided guidance on experimental design, and wrote most of the manuscript.

DECLARATION OF INTERESTS

The authors declare no competing interests.

Received: July 10, 2019
Revised: February 18, 2020
Accepted: March 28, 2020
Published: April 21, 2020

REFERENCES

Abbas, A.I., Sundiang, M.J.M., Henoch, B., Morton, M.P., Bolkan, S.S., Park, A.J., Harris, A.Z., Kellendonk, C., and Gordon, J.A. (2018). Somatostatin interneurons facilitate hippocampal-prefrontal synchrony and prefrontal spatial encoding. Neuron *100*, 926–939.e3.

Achim, A.M., Maziade, M., Raymond, E., Olivier, D., Mérette, C., and Roy, M.-A. (2011). How prevalent are anxiety disorders in schizophrenia? A meta-analysis and critical review on a significant association. Schizophr. Bull. *37*, 811–821.

Albaugh, M.D., Orr, C., Chaarani, B., Althoff, R.R., Allgaier, N., D'Alberto, N., Hudson, K., Mackey, S., Spechler, P.A., Banaschewski, T., et al. (2017). Inattention and reaction time variability are linked to ventromedial prefrontal volume in adolescents. Biol. Psychiatry *82*, 660–668.

Andrade, T.G., Zangrossi, H., Jr., and Graeff, F.G. (2013). The median raphe nucleus in anxiety revisited. J. Psychopharmacol. (Oxford) *27*, 1107–1115.

Arbogast, T., Ouagazzal, A.M., Chevalier, C., Kopanitsa, M., Afinowi, N., Migliavacca, E., Cowling, B.S., Birling, M.C., Champy, M.F., Reymond, A., and Herault, Y. (2016). Reciprocal effects on neurocognitive and metabolic phenotypes in mouse models of 16p11.2 deletion and duplication syndromes. PLoS Genet. *12*, e1005709.

Bains, R.S., Cater, H.L., Sillito, R.R., Chartsias, A., Sneddon, D., Concas, D., Keskivali-Bond, P., Lukins, T.C., Wells, S., Acevedo Arozena, A., et al. (2016). Analysis of individual mouse activity in group housed animals of different inbred strains using a novel automated home cage analysis system. Front. Behav. Neurosci. *10*, 106.

Bains, R.S., Wells, S., Sillito, R.R., Armstrong, J.D., Cater, H.L., Banks, G., and Nolan, P.M. (2018). Assessing mouse behaviour throughout the light/dark cycle using automated in-cage analysis tools. J. Neurosci. Methods *300*, 37–47.

Barak, B., and Feng, G. (2016). Neurobiology of social behavior abnormalities in autism and Williams syndrome. Nat. Neurosci. *19*, 647–655.

Barbas, H., and Blatt, G.J. (1995). Topographically specific hippocampal projections target functionally distinct prefrontal areas in the rhesus monkey. Hippocampus *5*, 511–533.

Barbey, A.K., Koenigs, M., and Grafman, J. (2011). Orbitofrontal contributions to human working memory. Cereb. Cortex *21*, 789–795.

Beasley, C.L., and Reynolds, G.P. (1997). Parvalbumin-immunoreactive neurons are reduced in the prefrontal cortex of schizophrenics. Schizophr. Res. *24*, 349–355.

Beasley, C.L., Zhang, Z.J., Patten, I., and Reynolds, G.P. (2002). Selective deficits in prefrontal cortical GABAergic neurons in schizophrenia defined by the presence of calcium-binding proteins. Biol. Psychiatry *52*, 708–715.

Bicks, L.K., Koike, H., Akbarian, S., and Morishita, H. (2015). Prefrontal cortex and social cognition in mouse and man. Front. Psychol. *6*, 1805.

Blumenthal, I., Ragavendran, A., Erdin, S., Klei, L., Sugathan, A., Guide, J.R., Manavalan, P., Zhou, J.Q., Wheeler, V.C., Levin, J.Z., et al. (2014). Transcriptional consequences of 16p11.2 deletion and duplication in mouse cortex and multiplex autism families. Am. J. Hum. Genet. *94*, 870–883.

Chang, X., Liu, Y., Hahn, C.G., Gur, R.E., Sleiman, P.M.A., and Hakonarson, H. (2017). RNA-seq analysis of amygdala tissue reveals characteristic expression profiles in schizophrenia. Transl. Psychiatry *7*, e1203.

Chau, B.K., Sallet, J., Papageorgiou, G.K., Noonan, M.P., Bell, A.H., Walton, M.E., and Rushworth, M.F. (2015). Contrasting roles for orbitofrontal cortex and amygdala in credit assignment and learning in macaques. Neuron *87*, 1106–1118.

Cole, M.W., Anticevic, A., Repovs, G., and Barch, D. (2011). Variable global dysconnectivity and individual differences in schizophrenia. Biol. Psychiatry *70*, 43–50.

Cooper, G.M., Coe, B.P., Girirajan, S., Rosenfeld, J.A., Vu, T.H., Baker, C., Williams, C., Stalker, H., Hamid, R., Hannig, V., et al. (2011). A copy number variation morbidity map of developmental delay. Nat. Genet. *43*, 838–846.

Csárdi, G., and Nepusz, T. (2006). The igraph software package for complex network research. InterJournal, 1695.

Dawson, N., Thompson, R.J., McVie, A., Thomson, D.M., Morris, B.J., and Pratt, J.A. (2012). Modafinil reverses phencyclidine-induced deficits in cognitive flexibility, cerebral metabolism, and functional brain connectivity. Schizophr. Bull. *38*, 457–474.

Dawson, N., Morris, B.J., and Pratt, J.A. (2013). Subanaesthetic ketamine treatment alters prefrontal cortex connectivity with thalamus and ascending subcortical systems. Schizophr. Bull. *39*, 366–377.

Dawson, N., Winchester, C.L., McVie, A., Thomsom, D., Hughes, Z.A., Dunlop, J., Brandon, N.J., Morris, B.J., and Pratt, J.A. (2014a). Disc1 mutation induced alterations in cerebral metabolism and in the response to acute subanaesthetic ketamine: a comparison of three different disc1 mutations. Schizophr. Res. *153* (*Suppl*), M9.

Dawson, N., Xiao, X., McDonald, M., Higham, D.J., Morris, B.J., and Pratt, J.A. (2014b). Sustained NMDA receptor hypofunction induces compromised neural systems integration and schizophrenia-like alterations in functional brain networks. Cereb. Cortex *24*, 452–464.

Dawson, N., Kurihara, M., Thomson, D.M., Winchester, C.L., McVie, A., Hedde, J.R., Randall, A.D., Shen, S., Seymour, P.A., Hughes, Z.A., et al. (2015a). Altered functional brain network connectivity and glutamate system function in transgenic mice expressing truncated Disrupted-in-Schizophrenia 1. Transl. Psychiatry *5*, e569.

Dawson, N., Morris, B.J., and Pratt, J.A. (2015b). Functional brain connectivity phenotypes for schizophrenia drug discovery. J. Psychopharmacol. (Oxford) *29*, 169–177.

Dias, R., Robbins, T.W., and Roberts, A.C. (1996). Dissociation in prefrontal cortex of affective and attentional shifts. Nature *380*, 69–72.

Dykiert, D., Der, G., Starr, J.M., and Deary, I.J. (2012). Sex differences in reaction time mean and intraindividual variability across the life span. Dev. Psychol. *48*, 1262–1276.

Elliott, R., Dolan, R.J., and Frith, C.D. (2000). Dissociable functions in the medial and lateral orbitofrontal cortex: evidence from human neuroimaging studies. Cereb. Cortex *10*, 308–317.

Elvevåg, B., Weinberger, D.R., Suter, J.C., and Goldberg, T.E. (2000). Continuous performance test and schizophrenia: a test of stimulus-response compatibility, working memory, response readiness, or none of the above? Am. J. Psychiatry *157*, 772–780.

Filges, I., Sparagana, S., Sargent, M., Selby, K., Schlade-Bartusiak, K., Lueder, G.T., Robichaux-Viehoever, A., Schlaggar, B.L., Shimony, J.S., and Shinawi, M. (2014). Brain MRI abnormalities and spectrum of neurological and clinical findings in three patients with proximal 16p11.2 microduplication. Am. J. Med. Genet. A. *164A*, 2003–2012.

Fleck, D.E., Sax, K.W., and Strakowski, S.M. (2001). Reaction time measures of sustained attention differentiate bipolar disorder from schizophrenia. Schizophr. Res. *52*, 251–259.

Fung, S.J., Webster, M.J., Sivagnanasundaram, S., Duncan, C., Elashoff, M., and Weickert, C.S. (2010). Expression of interneuron markers in the dorsolateral prefrontal cortex of the developing human and in schizophrenia. Am. J. Psychiatry *167*, 1479–1488.

Giegling, I., Hosak, L., Mossner, R., Serretti, A., Bellivier, F., Claes, S., Collier, D.A., Corrales, A., DeLisi, L.E., Gallo, C., et al. (2017). Genetics of schizophrenia: a consensus paper of the WFSBP Task Force on Genetics. World J. Biol. Psychiatry *18*, 492–505.

Godsil, B.P., Kiss, J.P., Spedding, M., and Jay, T.M. (2013). The hippocampal-prefrontal pathway: the weak link in psychiatric disorders? Eur. Neuropsychopharmacol. *23*, 1165–1181.

Golzio, C., Willer, J., Talkowski, M.E., Oh, E.C., Taniguchi, Y., Jacquemont, S., Reymond, A., Sun, M., Sawa, A., Gusella, J.F., et al. (2012). KCTD13 is a major

driver of mirrored neuroanatomical phenotypes of the 16p11.2 copy number variant. Nature *485*, 363–367.

Goodwill, H.L., Manzano-Nieves, G., LaChance, P., Teramoto, S., Lin, S., Lopez, C., Stevenson, R.J., Theyel, B.B., Moore, C.I., Connors, B.W., and Bath, K.G. (2018). Early life stress drives sex-selective impairment in reversal learning by affecting parvalbumin interneurons in orbitofrontal cortex of mice. Cell Rep. *25*, 2299–2307.e4.

Grabenhorst, F., Báez-Mendoza, R., Genest, W., Deco, G., and Schultz, W. (2019). Primate amygdala neurons simulate decision processes of social partners. Cell *177*, 986–998.e15.

Green, M.F., Horan, W.P., and Lee, J. (2015). Social cognition in schizophrenia. Nat. Rev. Neurosci. *16*, 620–631.

Guo, X., Li, J., Wang, J., Fan, X., Hu, M., Shen, Y., Chen, H., and Zhao, J. (2014). Hippocampal and orbital inferior frontal gray matter volume abnormalities and cognitive deficit in treatment-naive, first-episode patients with schizophrenia. Schizophr. Res. *152*, 339–343.

Hashimoto, T., Arion, D., Unger, T., Maldonado-Avilés, J.G., Morris, H.M., Volk, D.W., Mirnics, K., and Lewis, D.A. (2008). Alterations in GABA-related transcriptome in the dorsolateral prefrontal cortex of subjects with schizophrenia. Mol. Psychiatry *13*, 147–161.

Hoftman, G.D., Volk, D.W., Bazmi, H.H., Li, S., Sampson, A.R., and Lewis, D.A. (2015). Altered cortical expression of GABA-related genes in schizophrenia: illness progression vs developmental disturbance. Schizophr. Bull. *41*, 180–191.

Homayoun, H., and Moghaddam, B. (2008). Orbitofrontal cortex neurons as a common target for classic and glutamatergic antipsychotic drugs. Proc. Natl. Acad. Sci. USA *105*, 18041–18046.

Horev, G., Ellegood, J., Lerch, J.P., Son, Y.-E.E., Muthuswamy, L., Vogel, H., Krieger, A.M., Buja, A., Henkelman, R.M., Wigler, M., and Mills, A.A. (2011). Dosage-dependent phenotypes in models of 16p11.2 lesions found in autism. Proc. Natl. Acad. Sci. USA *108*, 17076–17081.

Iversen, S.D., and Mishkin, M. (1970). Perseverative interference in monkeys following selective lesions of the inferior prefrontal convexity. Exp. Brain Res. *11*, 376–386.

Johnson, A.W., Jaaro-Peled, H., Shahani, N., Sedlak, T.W., Zoubovsky, S., Burruss, D., Emiliani, F., Sawa, A., and Gallagher, M. (2013). Cognitive and motivational deficits together with prefrontal oxidative stress in a mouse model for neuropsychiatric illness. Proc. Natl. Acad. Sci. USA *110*, 12462–12467.

Johnston, H.M., and Morris, B.J. (1994). NMDA and nitric oxide increase microtubule-associated protein 2 gene expression in hippocampal granule cells. J. Neurochem. *63*, 379–382.

Joshi, D., Catts, V.S., Olaya, J.C., and Shannon Weickert, C. (2015). Relationship between somatostatin and death receptor expression in the orbital frontal cortex in schizophrenia: a postmortem brain mRNA study. NPJ Schizophr. *1*, 14004.

Kim, C.H., Hvoslef-Eide, M., Nilsson, S.R., Johnson, M.R., Herbert, B.R., Robbins, T.W., Saksida, L.M., Bussey, T.J., and Mar, A.C. (2015). The continuous performance test (rCPT) for mice: a novel operant touchscreen test of attentional function. Psychopharmacology (Berl.) *232*, 3947–3966.

Kirov, G., Rees, E., Walters, J.T.R., Escott-Price, V., Georgieva, L., Richards, A.L., Chambert, K.D., Davies, G., Legge, S.E., Moran, J.L., et al. (2014). The penetrance of copy number variations for schizophrenia and developmental delay. Biol. Psychiatry *75*, 378–385.

Knoll, M., Arnett, K., and Hertza, J. (2018). 16p11.2 Microduplication and associated symptoms: a case study. Appl. Neuropsychol. Child *7*, 374–379.

Lacerda, A.L., Hardan, A.Y., Yorbik, O., Vemulapalli, M., Prasad, K.M., and Keshavan, M.S. (2007). Morphology of the orbitofrontal cortex in first-episode schizophrenia: relationship with negative symptomatology. Prog. Neuropsychopharmacol. Biol. Psychiatry *31*, 510–516.

Liu, S.K., Hwu, H.-G., and Chen, W.J. (1997). Clinical symptom dimensions and deficits on the Continuous Performance Test in schizophrenia. Schizophr. Res. *25*, 211–219.

Malvaez, M., Shieh, C., Murphy, M.D., Greenfield, V.Y., and Wassum, K.M. (2019). Distinct cortical-amygdala projections drive reward value encoding and retrieval. Nat. Neurosci. *22*, 762–769.

Manoach, D.S. (2003). Prefrontal cortex dysfunction during working memory performance in schizophrenia: reconciling discrepant findings. Schizophr. Res. *60*, 285–298.

Mar, A.C., Horner, A.E., Nilsson, S.R., Alsiö, J., Kent, B.A., Kim, C.H., Holmes, A., Saksida, L.M., and Bussey, T.J. (2013). The touchscreen operant platform for assessing executive function in rats and mice. Nat. Protoc. *8*, 1985–2005.

Marighetto, A., Valerio, S., Philippin, J.N., Bertaina-Anglade, V., Drieu la Rochelle, C., Jaffard, R., and Morain, P. (2008). Comparative effects of the dopaminergic agonists piribedil and bromocriptine in three different memory paradigms in rodents. J. Psychopharmacol. (Oxford) *22*, 511–521.

Marshall, C.R., Howrigan, D.P., Merico, D., Thiruvahindrapuram, B., Wu, W., Greer, D.S., Antaki, D., Shetty, A., Holmans, P.A., Pinto, D., et al.; Psychosis Endophenotypes International Consortium; CNV and Schizophrenia Working Groups of the Psychiatric Genomics Consortium (2017). Contribution of copy number variants to schizophrenia from a genome-wide study of 41,321 subjects. Nat. Genet. *49*, 27–35.

Martin-Brevet, S., Rodríguez-Herreros, B., Nielsen, J.A., Moreau, C., Modenato, C., Maillard, A.M., Pain, A., Richetin, S., Jønch, A.E., Qureshi, A.Y., et al.; 16p11.2 European Consortium; Simons Variation in Individuals Project (VIP) Consortium (2018). Quantifying the effects of 16p11.2 copy number variants on brain structure: a multisite genetic-first study. Biol. Psychiatry *84*, 253–264.

Mazzucchelli, C., and Brambilla, R. (2000). Ras-related and MAPK signalling in neuronal plasticity and memory formation. Cell. Mol. Life Sci. *57*, 604–611.

McCarthy, S.E., Makarov, V., Kirov, G., Addington, A.M., McClellan, J., Yoon, S., Perkins, D.O., Dickel, D.E., Kusenda, M., Krastoshevsky, O., et al.; Wellcome Trust Case Control Consortium (2009). Microduplications of 16p11.2 are associated with schizophrenia. Nat. Genet. *41*, 1223–1227.

Mevik, B.-H., Wehrens, R., and Liland, K. (2019). Package 'pls': Partial Least Squares and Principle Component Regression. R package version 27-2. https://cran.r-project.org/web/packages/pls/pls.pdf.

Meyer-Lindenberg, A.S., Olsen, R.K., Kohn, P.D., Brown, T., Egan, M.F., Weinberger, D.R., and Berman, K.F. (2005). Regionally specific disturbance of dorsolateral prefrontal-hippocampal functional connectivity in schizophrenia. Arch. Gen. Psychiatry *62*, 379–386.

Millan, M.J., and Bales, K.L. (2013). Towards improved animal models for evaluating social cognition and its disruption in schizophrenia: the CNTRICS initiative. Neurosci. Biobehav. Rev. *37* (*9 Pt B*), 2166–2180.

Mohammad, H., Marchisella, F., Ortega-Martinez, S., Hollos, P., Eerola, K., Komulainen, E., Kulesskaya, N., Freemantle, E., Fagerholm, V., Savontaus, E., et al. (2018). JNK1 controls adult hippocampal neurogenesis and imposes cell-autonomous control of anxiety behaviour from the neurogenic niche. Mol. Psychiatry *23*, 362–374.

Morris, H.M., Hashimoto, T., and Lewis, D.A. (2008). Alterations in somatostatin mRNA expression in the dorsolateral prefrontal cortex of subjects with schizophrenia or schizoaffective disorder. Cereb. Cortex *18*, 1575–1587.

Nakamura, M., Nestor, P.G., Levitt, J.J., Cohen, A.S., Kawashima, T., Shenton, M.E., and McCarley, R.W. (2008). Orbitofrontal volume deficit in schizophrenia and thought disorder. Brain *131*, 180–195.

Nilsson, S.R., Fejgin, K., Gastambide, F., Vogt, M.A., Kent, B.A., Nielsen, V., Nielsen, J., Gass, P., Robbins, T.W., Saksida, L.M., et al. (2016). Assessing the cognitive translational potential of a mouse model of the 22q11.2 microdeletion syndrome. Cereb. Cortex *26*, 3991–4003.

Openshaw, R.L., Thomson, D.M., Thompson, R., Penninger, J.M., Pratt, J.A., Morris, B.J., and Dawson, N. (2020). Map2k7 haploinsufficiency induces brain imaging endophenotypes and behavioral phenotypes relevant to schizophrenia. Schizophr. Bull. *46*, 211–223.

Pantazopoulos, H., Wiseman, J.T., Markota, M., Ehrenfeld, L., and Berretta, S. (2017). Decreased numbers of somatostatin-expressing neurons in the

amygdala of subjects with bipolar disorder or schizophrenia: relationship to circadian rhythms. Biol. Psychiatry *81*, 536–547.

Pantelis, C., Velakoulis, D., McGorry, P.D., Wood, S.J., Suckling, J., Phillips, L.J., Yung, A.R., Bullmore, E.T., Brewer, W., Soulsby, B., et al. (2003). Neuroanatomical abnormalities before and after onset of psychosis: a cross-sectional and longitudinal MRI comparison. Lancet *361*, 281–288.

Pratt, J.A., and Morris, B.J. (2015). The thalamic reticular nucleus: a functional hub for thalamocortical network dysfunction in schizophrenia and a target for drug discovery. J. Psychopharmacol. (Oxford) *29*, 127–137.

Pratt, J.A., Morris, B.J., and Dawson, N. (2018). Deconstructing schizophrenia: advances in preclinical models for biomarker identification. Curr. Top. Behav. Neurosci. *40*, 295–323.

Pratt, J.A., Winchester, C., Dawson, N., and Morris, B.J. (2012). Advancing schizophrenia drug discovery: optimizing rodent models to bridge the translational gap. Nat. Rev. Drug Discov. *11*, 560–579.

R Core Team (2018). R: A Language and Environment for Statistical Computing. (R Foundation for Statistical Computing).

Rees, E., Walters, J.T.R., Georgieva, L., Isles, A.R., Chambert, K.D., Richards, A.L., Mahoney-Davies, G., Legge, S.E., Moran, J.L., McCarroll, S.A., et al. (2014). Analysis of copy number variations at 15 schizophrenia-associated loci. Br. J. Psychiatry *204*, 108–114.

Richter, M., Murtaza, N., Scharrenberg, R., White, S.H., Johanns, O., Walker, S., Yuen, R.K.C., Schwanke, B., Bedürftig, B., Henis, M., et al. (2019). Altered TAOK2 activity causes autism-related neurodevelopmental and cognitive abnormalities through RhoA signaling. Mol. Psychiatry *24*, 1329–1350.

Roberts, A.C., Tomic, D.L., Parkinson, C.H., Roeling, T.A., Cutter, D.J., Robbins, T.W., and Everitt, B.J. (2007). Forebrain connectivity of the prefrontal cortex in the marmoset monkey (*Callithrix jacchus*): an anterograde and retrograde tract-tracing study. J. Comp. Neurol. *502*, 86–112.

Rosenfeld, J.A., Coppinger, J., Bejjani, B.A., Girirajan, S., Eichler, E.E., Shaffer, L.G., and Ballif, B.C. (2010). Speech delays and behavioral problems are the predominant features in individuals with developmental delays and 16p11.2 microdeletions and microduplications. J. Neurodev. Disord. *2*, 26–38.

Ross, R.S., LoPresti, M.L., Schon, K., and Stern, C.E. (2013). Role of the hippocampus and orbitofrontal cortex during the disambiguation of social cues in working memory. Cogn. Affect. Behav. Neurosci. *13*, 900–915.

Rubinov, M., and Bullmore, E. (2013). Schizophrenia and abnormal brain network hubs. Dialogues Clin. Neurosci. *15*, 339–349.

Sakurai, T., Gamo, N.J., Hikida, T., Kim, S.-H., Murai, T., Tomoda, T., and Sawa, A. (2015). Converging models of schizophrenia–Network alterations of prefrontal cortex underlying cognitive impairments. Prog. Neurobiol. *134*, 178–201.

Salvador, R., Sarró, S., Gomar, J.J., Ortiz-Gil, J., Vila, F., Capdevila, A., Bullmore, E., McKenna, P.J., and Pomarol-Clotet, E. (2010). Overall brain connectivity maps show cortico-subcortical abnormalities in schizophrenia. Hum. Brain Mapp. *31*, 2003–2014.

Sanfilipo, M., Lafargue, T., Rusinek, H., Arena, L., Loneragan, C., Lautin, A., Feiner, D., Rotrosen, J., and Wolkin, A. (2000). Volumetric measure of the frontal and temporal lobe regions in schizophrenia: relationship to negative symptoms. Arch. Gen. Psychiatry *57*, 471–480.

Schirmbeck, F., Mier, D., Esslinger, C., Rausch, F., Englisch, S., Eifler, S., Meyer-Lindenberg, A., Kirsch, P., and Zink, M. (2015). Increased orbitofrontal cortex activation associated with "pro-obsessive" antipsychotic treatment in patients with schizophrenia. J. Psychiatry Neurosci. *40*, 89–99.

Schneider, C., A., Rasband, W.S., and Eliceiri, K.W. (2012). NIH Image to ImageJ: 25 years of image analysis. Nat. Methods. *9*, 671–675.

Schobel, S.A., Kelly, M.A., Corcoran, C.M., Van Heertum, K., Seckinger, R., Goetz, R., Harkavy-Friedman, J., and Malaspina, D. (2009). Anterior hippocampal and orbitofrontal cortical structural brain abnormalities in association with cognitive deficits in schizophrenia. Schizophr. Res. *114*, 110–118.

Selcher, J.C., Nekrasova, T., Paylor, R., Landreth, G.E., and Sweatt, J.D. (2001). Mice lacking the ERK1 isoform of MAP kinase are unimpaired in emotional learning. Learn. Mem. *8*, 11–19.

Shin, L.M., and Liberzon, I. (2010). The neurocircuitry of fear, stress, and anxiety disorders. Neuropsychopharmacology *35*, 169–191.

Shin, Y.S., Kim, S.N., Shin, N.Y., Jung, W.H., Hur, J.W., Byun, M.S., Jang, J.H., An, S.K., and Kwon, J.S. (2013). Increased intra-individual variability of cognitive processing in subjects at risk mental state and schizophrenia patients. PLoS ONE *8*, e78354.

Sigurdsson, T., Stark, K.L., Karayiorgou, M., Gogos, J.A., and Gordon, J.A. (2010). Impaired hippocampal-prefrontal synchrony in a genetic mouse model of schizophrenia. Nature *464*, 763–767.

Silbersweig, D.A., Stern, E., Frith, C., Cahill, C., Holmes, A., Grootoonk, S., Seaward, J., McKenna, P., Chua, S.E., Schnorr, L., et al. (1995). A functional neuroanatomy of hallucinations in schizophrenia. Nature *378*, 176–179.

Stefanoska, K., Bertz, J., Volkerling, A.M., van der Hoven, J., Ittner, L.M., and Ittner, A. (2018). Neuronal MAP kinase p38α inhibits c-Jun N-terminal kinase to modulate anxiety-related behaviour. Sci. Rep. *8*, 14296.

Stefansson, H., Rujescu, D., Cichon, S., Pietiläinen, O.P.H., Ingason, A., Steinberg, S., Fossdal, R., Sigurdsson, E., Sigmundsson, T., Buizer-Voskamp, J.E., et al.; GROUP (2008). Large recurrent microdeletions associated with schizophrenia. Nature *455*, 232–236.

Stefansson, H., Meyer-Lindenberg, A., Steinberg, S., Magnusdottir, B., Morgen, K., Arnarsdottir, S., Bjornsdottir, G., Walters, G.B., Jonsdottir, G.A., Doyle, O.M., et al. (2014). CNVs conferring risk of autism or schizophrenia affect cognition in controls. Nature *505*, 361–366.

Steinman, K.J., Spence, S.J., Ramocki, M.B., Proud, M.B., Kessler, S.K., Marco, E.J., Green Snyder, L., D'Angelo, D., Chen, Q., Chung, W.K., and Sherr, E.H.; Simons VIP Consortium (2016). 16p11.2 deletion and duplication: Characterizing neurologic phenotypes in a large clinically ascertained cohort. Am. J. Med. Genet. A. *170*, 2943–2955.

Sumner, P.J., Bell, I.H., and Rossell, S.L. (2018). A systematic review of the structural neuroimaging correlates of thought disorder. Neurosci. Biobehav. Rev. *84*, 299–315.

Vassos, E., Collier, D.A., Holden, S., Patch, C., Rujescu, D., St Clair, D., and Lewis, C.M. (2010). Penetrance for copy number variants associated with schizophrenia. Hum. Mol. Genet. *19*, 3477–3481.

Weiss, L.A., Shen, Y., Korn, J.M., Arking, D.E., Miller, D.T., Fossdal, R., Saemundsen, E., Stefansson, H., Ferreira, M.A., Green, T., et al.; Autism Consortium (2008). Association between microdeletion and microduplication at 16p11.2 and autism. N. Engl. J. Med. *358*, 667–675.

Wisden, W., and Morris, B.J. (1994). In Situ Hybridisation Protocols for the Brain (Academic Press).

Wisden, W., Errington, M.L., Williams, S., Dunnett, S.B., Waters, C., Hitchcock, D., Evan, G., Bliss, T.V.P., and Hunt, S.P. (1990). Differential expression of immediate early genes in the hippocampus and spinal cord. Neuron *4*, 603–614.

Wold, S. (1995). PLS for multivariate linear modelling. In Chemometric Methods in Molecular Design, H. van de Waterbeemd, ed. (VCH), pp. 195–218.

Wold, S., Sjostrom, M., and Eriksson, L. (2001). PLS-regression: a basic tool of chemometrics. Chemom. Intell. Lab. Syst. *58*, 109–130.

Zald, D.H., McHugo, M., Ray, K.L., Glahn, D.C., Eickhoff, S.B., and Laird, A.R. (2014). Meta-analytic connectivity modeling reveals differential functional connectivity of the medial and lateral orbitofrontal cortex. Cereb. Cortex *24*, 232–248.

Zheng, X., Bei, J.-X., Xu, H., Lee, J., Chong, S.-A., Sim, K., Liany, H., Shyong, T.E., Liu, T., Foo, J.N., et al. (2013). The association between rare large duplication of 16p11.2 and schizophrenia in the Singaporean Chinese population. Schizophr. Res. *146*, 368–369.

Zhou, Y., Wang, Z., Zuo, X.N., Zhang, H., Wang, Y., Jiang, T., and Liu, Z. (2014). Hyper-coupling between working memory task-evoked activations and amplitude of spontaneous fluctuations in first-episode schizophrenia. Schizophr. Res. *159*, 80–89.

STAR★METHODS

KEY RESOURCES TABLE

REAGENT or RESOURCE	SOURCE	IDENTIFIER
Chemicals, Peptides, and Recombinant Proteins		
35S-dATP	PerkinElmer	NEG034H
Deoxy-D-glucose, 2-[1-^{14}C]	American Radiolabeled Chemicals Inc.	ARC0111A
paraformaldehyde	Merck	1040051000
terminal deoxynucleotidyl transferase	ThermoFisher	EP0162
standard saline citrate buffer	Sigma	C-2488
poly-L-Lysine	Sigma	P-1524
Experimental Models: Organisms/Strains		
Dp(7Slx1b-Sept1)5Aam strain (16p11.2 DUP mice)	The Jackson Laboratory	JAX: 016915
Oligonucleotides		
Pvalb: AGTGGAGAATTCTTCAACCCCAATCTTGC CGTCCCCATCCTTGTC	Sigma	N/A
GAD1: CCTGCACACATCTGGTTGCATCCTTGGA GTATACCCTTTTCCTTG	Sigma	N/A
SST:CAAATCCTCGGGCTCCAGGGCATCATTCT CTGTCTGGTTGGGCTC	Sigma	N/A
Calb1:AATTCCTATTTTTCCATCATCTCTCTGTC CATATTGATCCACAAA	Sigma	N/A
Calb2:CTGTTGGATGTTCATCTCCTTCTTGT TCTTCTCATACAGATCCT	Sigma	N/A
Recombinant DNA		
Software and Algorithms		
ImageJ	Schneider et al., 2012	https://imagej.nih.gov/ij/
ABETII touch software package (rCPT)	Campden Instruments LTD	
R	R Core team, 2018	http://www.r-project.org
Pls Package	Mevik et al., 2019	https://cran.r-project.org/web/packages/pls/pls.pdf
EthoVision® XT software	Noldus Information Technology	
igraph Package	Csárdi and Nepusz, 2006	https://igraph.org/redirect.html
Other		
14-C autoradiography standards	American Radiolabeled Chemicals, Inc.	ARC0146R

LEAD CONTACT AND MATERIALS AVAILABILITY

Materials Availability Statement: There are no newly generated materials or tools associated with this report, and this study did not generate new unique reagents. The GM mouse strain is available from Jackson Laboratories.

Further information and requests for resources and reagents should be directed to and will be fulfilled by the Lead Contact: Brian J. Morris (brian.morris@glasgow.ac.uk)

EXPERIMENTAL MODEL AND SUBJECT DETAILS

Animals

Mice hemizygous for the 0.44-Mb region of mouse chromosome 7, syntenic to the human 16p11.2 duplication, were generated by Mills and colleagues (Horev et al., 2011) (Jackson Laboratory stock No. 016915), and backcrossed onto a C57BL/6 background to generate the experimental mice used in these studies (16p11.2 DUP mice). 16p11.2 DUP mice, and littermate wild-type (WT) controls, were housed on site for a minimum of 2 weeks prior to experimental use, group housed under standard conditions, with food and

water *ad libitum*, under reversed light/dark cycle (lights off at 10am). Mice were used at 63-79 days old for functional imaging, at 49-63 days old for simple behaviors and *in situ* hybridization, and as detailed for cognitive behaviors, and were tested in randomized order. All work was approved by the relevant University Animal Welfare and Ethics Review Board (AWERB) and conducted in accordance with the UK Animals (Scientific Procedures) Act 1986.

METHOD DETAILS

In Situ Hybridization

Group size: WT, n = 12 (6 male, 6 female) and 16p11.2 DUP, n = 12 (6 male, 6 female) was estimated, based on our previous experiments with GM mice, to provide 99% power to detect an effect at $p < 0.05$ (Minitab). Regional mRNA expression was monitored by *in situ* hybridization according to our published methods (Wisden and Morris, 1994) using ^{35}S-labeled 45-mer oligonucleotide probes complementary to target mRNAs. 20 μm frozen cryostat sections were mounted on microscope slides coated with poly-L-Lysine (Sigma) and fixed for 10 minutes in 4% paraformaldehyde (Sigma) on ice. Oligonucleotides were 3′end-labeled with ^{35}S-dATP using terminal deoxynucleotidyl transferase (ThermoFisher). Hybridization with sections was performed at 42°C overnight in a humidified chamber, and the next day sections were washed for 1 hour in standard saline citrate buffer (Sigma) at 55°C, before being dehydrated in ethanol. Specificity of labeling was assessed using competition controls (25x excess of unlabeled oligonucleotide) (Johnston and Morris, 1994; Wisden et al., 1990; Wisden and Morris, 1994). Autoradiographic signal intensity was measured using ImageJ (Schneider et al., 2012), while blind to the genotype and sex of the samples.

14C-2-Deoxyglucose Imaging

Group size: WT, n = 10 (6 male, 5 female) and 16p11.2 DUP, n = 10 (6 male, 5 female) was estimated, based on our previous experiments with GM mice, to provide 85% power to detect an effect at $p < 0.05$ (Minitab). 14C-2-deoxyglucose (14C-2-DG) functional brain imaging was conducted in accordance with previously published protocols (Dawson et al., 2013, 2012). Autoradiographic signal intensity was measured using a MCID system, while blind to the sex and genotype of the samples.

Network Analysis using Graph Theory Algorithms

Using network science/graph theory algorithms, global functional brain network structure properties and regional centrality analysis were analyzed using the igraph package (Csárdi and Nepusz, 2006) in R (R Core Team, 2018). The application of brain network analysis to 14C-2-DG brain imaging data has previously been described in detail (Dawson et al., 2015b, 2013, 2012). The algorithms applied here allow us to define the properties of functional brain networks at the global scale (mean degree ($< k >$), average path length (Lp) and clustering coefficient (Cp)) and to also define the importance of each brain region in the context of the whole brain network (centrality analysis; degree (ki), betweenness (Bc) and Eigenvector (Ec)).

Partial Least-Squares Regression (PLSR)

The application of PLSR to functional 14C-2DG brain imaging data and it interpretation has been considered elsewhere in detail (Dawson et al., 2013, 2012). Data were analyzed using the Pls package (Mevik et al., 2019) in R. Significant inter-regional connectivity to the "seed" RoI being analyzed was considered to exist within the experimental group if the lower bound of the 95% confidence interval (CI) of the variable importance to the projection (VIP) statistic (estimated by jack-knifing) exceeded the 1.0 threshold. Significantly altered connectivity in 16p11.2 DUP mice was determined by statistical comparison of the VIP statistic between experimental groups through the calculation of the standardized z-score, with a z-score < -2.98 considered to be significant. Significantly lost connectivity was confirmed by a 95% CI of the VIP > 1.0 in WT mice that was not present in 16p11.2 DUP mice (95% CI lower bound VIP < 1.0).

Using PLSR Analysis to Define Altered Relationships between Regional Cerebral Metabolism and Locomotor Activity (LMA) in 16p11.2 DUP Mice

To define the relationship between regional cerebral metabolism and LMA in experimental animals we employed the partial least-squares regression (PLSR) algorithm, which allows the quantification of the contribution of multiple, collinear explanatory "predictor" variables (X variables, in this case regional local cerebral glucose utilization) to one dependent variable (Y variable, in this case the relevant LMA measure). For a detailed overview of PLSR see Dawson et al. (2012); Wold (1995), and Wold et al. (2001). In this way the PLSR algorithm can model the relationship between regional cerebral metabolism and behavioral outcome measures.

Our data were analyzed using the PLSR package (Mevik et al., 2019) in R (R Core Team, 2018). The variable importance to the projection (VIP) statistic provides a summary of the relationship between the X and Y variables, with VIP values > 1 defined as making a large contribution to determining the values in X and Y (Wold et al., 2001). On this basis we calculated the VIP statistic for each brain region of interest (RoI) in relation to the four measures of LMA of interest (distance, velocity, movement frequency and movement duration) in the two experimental groups (WT and 16p11.2 DUP mice). Through a jack-knifing ("leave-one-out") procedure the standard deviation (SD) of the VIP statistic was estimated for each explanatory brain RoI and within each experimental group, and the lower bound of the 95% confidence interval (CI) for the VIP statistic determined. Within each experimental group the average 95% CI lower bound of the VIP statistic across the four locomotor measures was determined, with an average value > 1 considered to

indicate a substantial relationship between RoI metabolism and locomotor activity. Group differences in locomotor activity were determined through calculation of the average standardized z-score from each model (per LMA variable and genotype), with $z > 1.96$ or < -1.96 considered to be significant.

Gross Morphology

Brain size was determined by measuring the area of the brain autoradiograms gained in the 14C-2-deoxyglucose brain imaging study at 7 levels across the brain (Figure S6). We also analyzed the coronal sectional area of selected brain regions including the striatum, anterior thalamus (athal), medial thalamus (mthal) and the substantia nigra. In addition, we measured the cortical depth of several cortical regions, including the auditory cortex.

Open Field Arena

Group size: WT, n = 12 (6 male, 6 female) and 16p11.2 DUP, n = 12 (6 male, 6 female) was estimated, based on our previous experiments with GM mice, to provide 88% power to detect an effect at $p < 0.05$ (Minitab). Locomotor activity was assessed in an arena, made of black Perspex (size 40 × 40 × 40cm), semi-permeable to infrared light, lit from below by infrared LEDs. Activity was monitored and recorded using an infrared-sensitive digital camera (Sony) and EthoVision® XT software (Noldus Information Technology). Each mouse was placed initially in the center of each arena. All animals were tested for 60 minutes, with no prior habituation period

Elevated Plus Maze

Group size: WT, n = 12 (6 male, 6 female) and 16p11.2 DUP, n = 12 (6 male, 6 female) was estimated, based on our previous experiments with GM mice, to provide 80% power to detect an effect at $p < 0.05$ (Minitab). Plus maze apparatus consisted of two opposing enclosed, dark arms (30 cm x 6 cm) and two opposing open light arms (30 cm x 6 cm). The mouse was placed in center of the maze and allowed to freely move for 5 minutes. An overhead infra-red detecting camera tracked and analyzed activity. Data were analyzed using EthoVision Video Tracking System (Noldus Information Technology, Leesburg, VA).

PPI

Group size: WT, n = 12 (6 male, 6 female) and 16p11.2 DUP, n = 12 (6 male, 6 female) was estimated, based on our previous experiments with GM mice, to provide 92% power to detect an effect at $p < 0.05$ (Minitab). Using SR-LAB chambers (San Diego Instruments, San Diego, CA) as previously described (Openshaw et al., 2020), a startle curve (random presentation of 60 trials of 65dB, 69dB, 73dB, 77dB, 85dB, 90dB, 100dB, 110dB, 120dB - full spectrum white noise) was obtained. Pre-pulse inhibition determination involved random presentation of 120dB startle with 4, 8 and 16 db above a background dB level of 65dB (full spectrum white noise). % PPI was calculated as startle reactivity at 120 dB – startle reactivity with prepulse) / startle reactivity at 120 dB x 100).

N Back Radial Maze Task

Group size: WT, n = 12 (6 male, 6 female) and 16p11.2 DUP, n = 12 (6 male, 6 female) was estimated, based on our previous experiments with GM mice, to provide 80% power to detect an effect at $p < 0.05$ (Minitab). The N-back test was performed as described in Marighetto et al. (2008) using 6 arms from an automated 8 arm radial mazes (Med Associates Inc., St Albans, Vermont), with an automated pellet dispenser delivering a single reward pellet (Test Diet, formula 5TUL 14mg), at the end of each arm. The configuration and procedure is shown schematically in Figure S1. The 6 arms used were counterbalanced across groups to avoid any confounds due to inherent bias in the mazes. Following habituation (3 days of free access to the maze where all arms were accessible and 2 pellets placed in the food hoppers at the end of each arm), the full test schedule of 23 trials began, incorporating equal numbers of trials for each value of N. The 6 arms were allocated to 1 of 3 pairs of arms (pair A, B and C) which were presented in a random order. Following an initial presentation of a given pair (free choice; rewarded) a reward was delivered only when the alternative arm was selected from that selected in the previous presentation of the arm pair. The N-back set was then constructed from the individual trial set by the number of intervening alternative arm pair presentations (Marighetto et al., 2008).

CPT

Group size: WT, n = 12 (6 male, 6 female) and 16p11.2 DUP, n = 12 (6 male, 6 female) was estimated, based on our previous experiments with GM mice, to provide 86% power to detect an effect at $p < 0.05$ (Minitab). The CPT was performed using Campden instruments mouse touchscreen operant boxes, running the ABETII touch software package. A 3 aperture horizontal mask allowed selection of 3 discrete sections of the touchscreen. The center panel presented the task stimulus. For correct responses, (YazooTM) strawberry milkshake, delivered at 70 μl, represented the reward, a tone played and the food reward hopper illuminated. Stimuli were either S+, which was rewarded following a response, or S-, which were punished following a response by a correction phase with repeated stimulus presentation until the response is correctly withheld. The configuration and procedure is shown schematically in Figure S1. Training was performed as described (Kim et al., 2015) with basal response learning (stage 1), stimulus-specific responding (stage 2), stimulus-specific responding and non-responding (stage 3), followed by increased cognitive load (e.g., increased S- stimuli; reduced stimulus presentation times (2 s, 1.5 s, 1 s; limited hold 2.5 s, 2 s, 1.5 s) in stages 4-6). Parameters were: Hit rate (HR) - the rate at which animals respond to correct S+ stimulus (HR = Hit/(Hit+Miss)); False alarm rate (FAR) - the rate at which animals

respond to the S- stimulus and is a composite score composed as follows: FAR = False alarm/(False alarm + Correct rejection); Sensitivity index (SI) - the perceptual discriminability between the S+ and S−; i.e., higher values indicate better visual discrimination (Kim et al., 2015); Responsivity index (RI) - the criterion or willingness to make responses, e.g., conservative = low RI values while liberal = high RI values (Kim et al., 2015; see erratum for correct formula). Note that this is the converse of the LnBeta index, where low values indicate more liberal responding strategies.

Home Cage Monitoring

Group size: WT, n = 15 (6 male, 9 female) and 16p11.2 DUP, n = 15 (6 male, 9 female) was estimated, based on our previous experiments with GM mice, to provide 93% power to detect an effect at $p < 0.05$ (Minitab). A radiofrequency identification (RFID) transponder (Biomark, UK) was implanted subcutaneously into the lower left abdominal quadrant under isofluorane anesthesia a minimum of 2 days before recording. Groups of 3 mice were then placed in Plexiglas IVC cages monitored by the Home Cage Analyzer (Actual Analytics Ltd, UK) (Bains et al., 2016, 2018) equipment for 1.5h prior to data acquisition in order to habituate the animals. Recording commenced at 10am and proceeded for 72h. Measures included: total distance traveled (mm), total number of antenna transitions, separation (mean Euclidean distance to closest cage-mate (mm)) and proximity (time spent < 75mm apart from cage-mates (s)).

QUANTIFICATION AND STATISTICAL ANALYSIS

The statistical details of experiments can be found in the figure legends and in Table S7. All data were tested for normality of distribution prior to the use of ANOVA (Minitab).

DATA AND CODE AVAILABILITY

This study did not generate searchable datasets or code.